

Surgical Anatomy of the Temporal Lobe



Jander Moreira Monteiro and Gustavo Rassier Isolan

1 Introduction

The temporal lobe is the most heterogeneous segment of the human brain. It is formed by many allocortex and limbic system structures. The mesocortex constitutes the delineation between the temporal isocortex and part of the limbic system. This region is a frequent site of origin for epileptic focus and brain tumors. Approximately 9% of all epilepsy cases are classified as temporal lobe epilepsy—the total prevalence of epilepsy may range from 4 to 57 cases per 1000 persons, being more prominent in developing and tropical countries. Temporal lobe epilepsy is recurrently refractory to antiepileptic drugs and is the most prevalent type of partial epilepsy suitable for surgery approaches [1].

Following the heterogeneity of the area, temporal lobe epilepsy presents in two different ways: neocortical and mesial temporal. The evaluation and surgical treatment for neocortical temporal lobe epilepsy resemble those used for extratemporal epilepsy in general. Meanwhile, the therapeutics for mesial temporal epilepsy are specific, mostly based on its distinguished physiopathological process: mesial temporal sclerosis, usually affecting the hippocampus [2].

Two established surgical interventions for mesial temporal epilepsy are anterior temporal lobectomy and the more conservative amygdalohippocampectomy. Our purpose is to present our findings regarding the microsurgical anatomy of the temporal lobe and the importance of this anatomy in selective amygdalohippocampectomy and relate it to the three main approaches to this procedure: transsylvian approach, Niemeyer's technique, and subtemporal technique. Also, as the title

J. M. Monteiro · G. R. Isolan (✉)

The Center for Advanced Neurology and Neurosurgery (CEANNE), Porto Alegre, RS, Brazil

Mackenzie Evangelical Faculty of Paraná (FEMPAR), Curitiba, PR, Brazil

suggests, we aim to describe and discuss the temporal white fibers and the relation of this subcortical anatomy with cortical and subcortical brain mapping, which is especially useful in glioma surgeries.

2 Surgical Anatomy

2.1 Temporal Lobe Limits

On the lateral surface, the temporal lobe is delineated superiorly by the posterior ramus of the Sylvian fissure and posteriorly by the lateral parietotemporal line. The parietotemporal line is an imaginary line extending from the impression of the parieto-occipital fissure to the preoccipital notch. The temporo-occipital line is another similar line that separates the temporal from the parietal lobe. This line runs from the end of the posterior ramus of the Sylvian fissure to the midpoint of the lateral parietotemporal line. The limit between the temporal and occipital lobes on the basal surface is delineated by a line that connects the preoccipital notch to the inferior end of the parieto-occipital fissure—the basal parietotemporal line. For a didactic purpose, these delineations worked well but are artificial and elusive regarding the biological reality [3] (Figs. 1, 2, 3, 4, 5, 6, 7, and 8).

2.2 Temporal Lobe Sulci

The principal sulci identified in the temporal lobe are the superior, middle, and inferior temporal sulci, angular, hippocampal, uncus, rhinal, and collateral sulci. The superior temporal sulcus extends from the anterior aspect of the lateral surface of the temporal pole to the angular gyrus and is the most consistent sulcus in morphology [4]. The middle temporal sulcus is parallel to the superior temporal sulcus and

Fig. 1 Lateral view of a left hemisphere with temporal sulci, gyri, and limits: 1—superior temporal gyri; 2—middle temporal gyri; 3—inferior temporal gyri; 4—superior temporal sulcus; 5—middle (inferior) temporal sulcus; 6—Sylvian (lateral) fissure; discontinued line—temporo-occipital line; continued line—parieto-occipital line

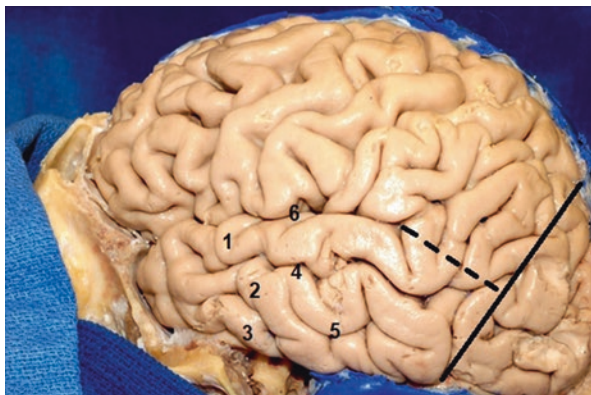
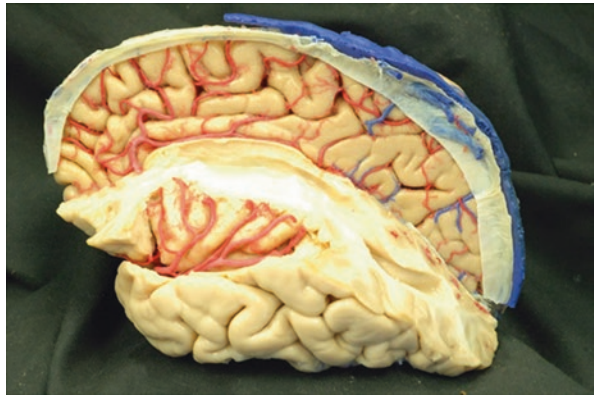


Fig. 2 Frontal operculum resection, exposing insular gyri and transverse temporal gyri



Fig. 3 The M2 branches of the middle cerebral artery travel in the sulci of the insular lobe, and, in the transylvian approach, surgeons work in the small windows delimited by these arterial branches



extends into the posterior portion of the inferior parietal lobule. The inferior temporal sulcus was not identified in all brains. It is present in about one-third of the individuals [5]. The inferior and middle temporal sulci were highly variable in morphology. The collateral sulcus was uninterrupted in 100% of the brains, while the inferior temporal sulcus was interrupted 100%. The rhinal sulcus is a short sulcus that was identified in all brains. The patterns of the interruptions in the sulcus of the temporal lobe and the terminations and connections of them are detailed in the study performed by Ono [5] (Figs. 1, 2, 3, 4, 5, 6, 7, and 8).

2.3 Temporal Gyri

The following principal gyri in the temporal lobe were identified: superior, middle, and inferior temporal gyri, fusiform, and parahippocampal gyri. The superior temporal gyrus (T1) can be divided into anterior, middle, and posterior segments. Three or four small gyri originate from the anterior portion of the superior temporal gyrus that goes into the depth of the anterior Sylvian fissure [6]. A sulcus divides this short

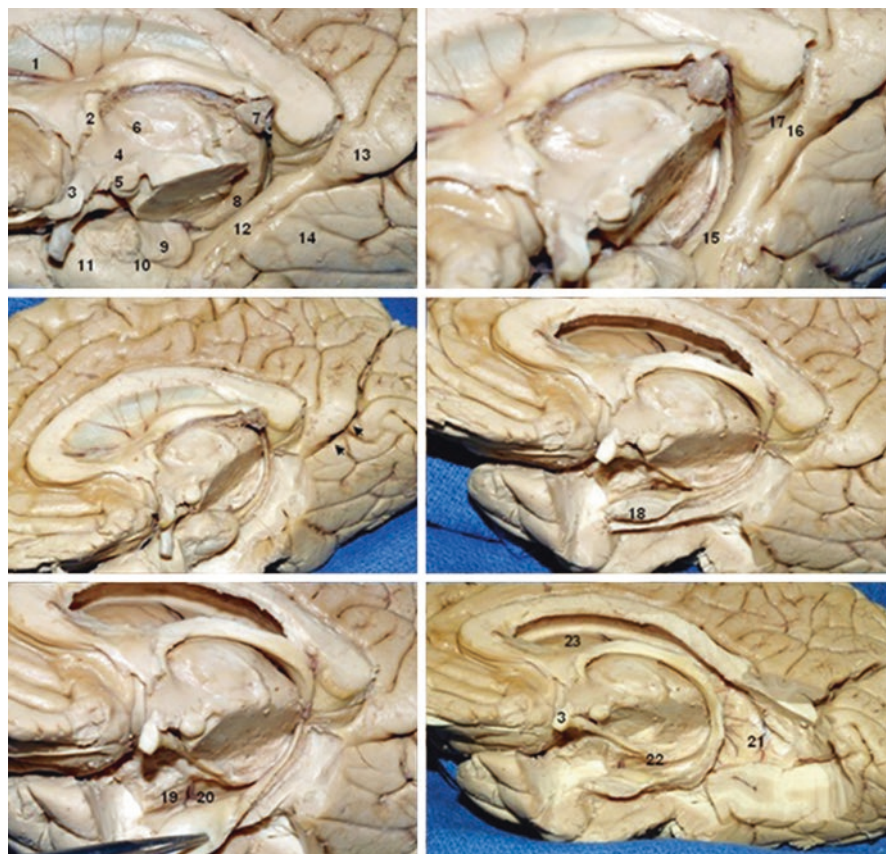


Fig. 4 Medial surface of a right-sided brain hemisphere: 1—septum pellucidum; 2—fornix (anterior column); 3—optic chiasm; 4—hippocampus; 5—mammillary body; 6—interthalamic adhesion; 7—pineal gland; 8—pulvinar nuclei (thalamus); 9—uncus; 10—uncal sulcus; 11—temporal pole; 12—parahippocampal gyrus; 13—cingulate gyrus; 14—lingual gyrus; 15—hippocampal sulcus; 16—isthmus; 17—fasciolar gyrus; 18—hippocampal head; 19—amygdala; 20—inferior choroid point; 21—ventricular atrium; 22—optic tract; 23—head of caudate nucleus; 24—anterior commissure; arrows—anterior calcarine sulcus

anterior gyrus from two bigger parallel gyri that run from the posterior part of the T1 to the ultimate end of the Sylvian fissure. These gyri sitting posteriorly are called transverse temporal gyri or Heschl gyri, containing the primary auditory cortex. The transverse gyrus of Heschl usually has two convolutions outlined by transverse sulci that run obliquely and are usually larger on the left side [4]. Behind the Heschl gyrus lies a triangular space called the *planum temporale*. The *planum temporale* is larger on the left side due to the left hemisphere dominance for speech [4]. This anatomical information is important because the length of the left Sylvian fissure is also larger than the right [4]. The superior surface of the superior temporal gyrus forms the temporal operculum. The middle temporal gyrus (T2) can be divided into

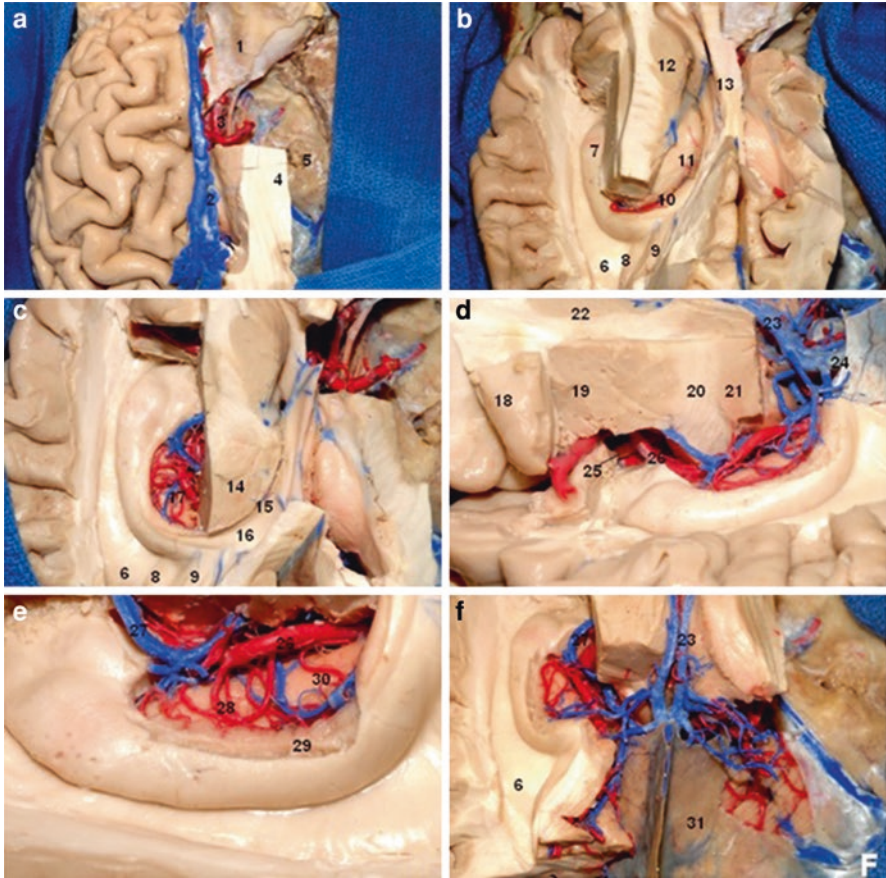


Fig. 5 Superior (a–c, f) and lateral (d, e) views of the hippocampus and surrounding areas: 1—orbital roof; 2—superior sagittal sinus; 3—internal carotid artery; 4—internal capsule; 5—middle fossa floor; 6—collateral triangle; 7—hippocampus; 8—calcar avis; 9—corpus callosum; 10—choroid fissure; 11—thalamus; 12—caudate nucleus head; 13—fornix; 14—pulvinar nuclei (thalamus); 15—choroid fissure (atrial portion); 16—crura fornices; 17—foramen of Monro; 18—short gyri of insula; 19—globus pallidus; 20—internal capsule; 21—pulvinar nuclei (thalamus); 22—caudate nucleus; 23—internal cerebral vein; 24—a vein of Galen; 25—oculomotor nerve; 26—posterior cerebral artery; 27—basal vein of Rosenthal; 28—middle hippocampal artery; 29—dentate gyrus; 30—posterior hippocampal artery; 31—cerebellar tentorium

anterior, middle, and posterior segments. It is separated from the superior temporal gyrus by the superior temporal sulcus and the inferior temporal gyrus by the middle temporal sulci/inferior temporal sulci. The three segments of the middle temporal sulci represent an interrupted sulcus that separates the middle and inferior temporal gyri. The middle segment of the middle temporal sulcus may be equivalent to the central part of the inferior temporal sulcus [5]. The anterior pole of the middle temporal gyrus is surrounded by the anterior part of the superior and inferior temporal gyri. The inferior temporal gyrus (T3) can be divided into anterior, middle, and

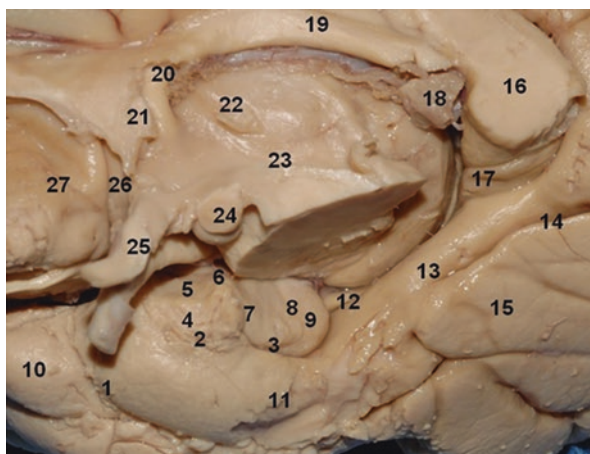
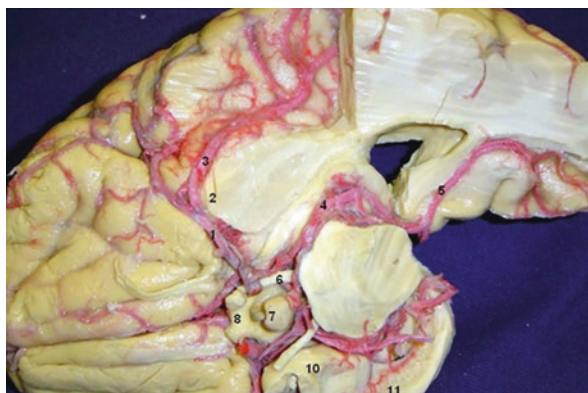


Fig. 6 Medial surface of a right-sided brain hemisphere: 1—rhinal sulcus; 2—uncus; 3—uncus sulcus; 4—gyrus ambiens; 5—semilunar gyrus; 6—entorhinal sulcus; 7—uncinate gyrus; 8—the band of Giacomini; 9—intralimbic gyrus; 10—temporal pole; 11—parahippocampal gyrus; 12—fimbria; 13—isthmus; 14—anterior calcarine sulcus; 15—lingual gyrus; 16—splenium of the corpus callosum; 17—fasciolar gyrus; 18—pineal gland; 19—the body of fornix; 20—anterior column of fornix; 21—anterior commissure; 22—interthalamic adhesion; 23—hypothalamic sulcus; 24—mammillary body; 25—optic chiasm; 26—paraterminal gyrus; 27—subcallosal gyrus

Fig. 7 Inferior view of the brain: 1—middle cerebral artery (M1 segment); 2—limen insulae; 4—middle cerebral artery (M2 segment); 5—calcarine artery (P4 segment); 6—oculomotor nerve; 7—pituitary gland; 8—optic chiasm; 9—internal carotid artery; 10—uncus; 11—dentate gyrus



posterior segments. It is separated from the lateral temporo-occipital gyrus by the inferior temporal sulcus. It is small compared to the other temporal gyri. The gyri of the temporal lobe convexity, except for the superior temporal gyrus, are difficult to identify due to their anatomical variability [4]. The fusiform gyrus (lateral temporo-occipital gyrus) (T4) is separated from the parahippocampal and lingual gyri by the collateral sulcus and has a “lazy” form. It has an anterior and posterior relation with the inferior temporal gyrus and the medial temporo-occipital gyrus. The

Fig. 8 Inferior view of brain's basal surface: 1—uncus; 2—gyrus ambiens; 3—parahippocampal gyrus; 4—rhinal sulcus; 5—fusiform gyrus; 6—collateral sulcus; 7—fusiform gyrus; 8—occipitotemporal sulcus; 9—inferior temporal gyrus; 10—anterior perforated substance; 11—optic chiasm; 12—oculomotor nerve; 13—pons; 14—olfactory tract; 15—gyrus rectus; 16—orbital gyri



parahippocampal (T5) gyrus sits between the uncus and the isthmus of the cingulate gyrus. It is separated from the fusiform gyrus by the collateral sulcus. The parahippocampal gyrus has a posterior segment called the subiculum. The hippocampal sulcus separates the subiculum from the hippocampus. The parahippocampal gyrus also has an anterior segment called the piriform lobe, formed by the uncus and entorhinal area. The uncus is separated from the parahippocampal gyrus by the uncal sulcus. The uncus has an anterior segment that covers the amygdala. This part is composed of the semilunar and ambient gyri, which are separated by the semilunar sulcus. The posterior segment of the uncus forms part of the hippocampus and the subiculum. The subiculum is divided into prosubiculum, subiculum proper, presubiculum, and parasubiculum. The entorhinal area does not have a precise delineation but is considered to extend into the posterior segment of the parahippocampal gyrus [7] (Figs. 1, 2, 3, 4, 5, 6, 7, and 8).

2.4 Considerations on Temporal Gyri and Sulci

Regarding the division of the brain in lobes, for a didactic purpose, this delineation worked well but is artificial and elusive regarding the biological reality [3]. It has not considered the complex and intricate white fiber tracts and fascicles that communicate with brain lobes, representing more accurately brain functions. Regarding temporal lobe sulci, the superior temporal sulcus is the most consistent

in morphology [4]. The inferior temporal sulcus is present in about one-third of the individuals [5]. The patterns of the interruptions analyzed in our dissection regarding the sulci of the temporal lobe and the terminations and connections are similar to the study performed by Ono [5].

The transverse gyrus of Heschl usually has two convolutions outlined by transverse sulci that run obliquely and are usually larger on the left side [4]. The planum temporale is larger on the left side due to the left hemisphere dominance for speech [4]. This anatomical information is important because the length of the left Sylvian fissure is also larger than the right [4]. The gyri of the temporal lobe convexity are, except for the superior temporal gyrus, difficult to identify due to their anatomical variability [4].

2.5 *Hippocampus*

The hippocampus forms an arc with an enlarged anterior extremity. The hippocampus belongs to the limbic lobe, separated from the adjacent cortex by the cingulate, subparietal, anterior calcarine, collateral, and rhinal sulci. Do these discontinuous sulci form the so-called? The limbic lobe is divided into limbic and intralimbic gyri [8]. The limbic gyrus is formed by the parahippocampal, cingulate, and subcallosal gyri. The intralimbic gyrus has two segments: anterior and superior. The anterior segment is part of the paraterminal gyrus and septal region and is referred to as the prehippocampal rudiment. The superior segment is the indusium griseum, a neuronal lamina on the corpus callosum extending to the hippocampus. The indusium griseum is covered by the medial and lateral longitudinal striae on each side of the midline. The limbic lobe can also be divided structurally in the allocortex (hippocampus, proximal part of the subiculum, and indusium griseum) and periallocortex (cingulate and parahippocampal gyri), which is a transitional cortex between the allocortex and isocortex [7].

Structurally, the hippocampus comprises two laminas that roll up inside the other—the Cornu Ammonis (hippocampus proper) and the gyrus dentatus. Both of them are allocortex. These structures are separated by the hippocampal sulcus, which is divided into vestigial and superficial hippocampal sulci. This last part can be seen on the temporal lobe surface. The Cornu Ammonis, from the intraventricular surface to the vestigial hippocampal sulcus, can be divided into six layers. These layers are alveus, stratum oriens, stratum pyramidale, stratum radiatum, stratum lacunosum, and stratum molecularis. The Cornu Ammonis has a heterogeneous structure in coronal sections and is divided into four fields: CA₁, CA₂, CA₃, and CA₄. CA₁ is the larger portion and continuous with the dentate gyrus, CA₂ has a dense and narrow stratum pyramidal, CA₃ corresponds to the genu of the Cornu Ammonis, and CA₄ is situated within the gyrus dentatus. CA₁ is considered the “vulnerable sector” to hypoxia, and CA₃ is the “resistant sector.” The gyrus dentatus, also known as gyrus involutus, is a concave lamina that envelopes CA₄. It is formed by three layers: stratum granulosum, stratum molecular, and polymorphic

layer. It is separated from the Cornu Ammonis by the vestigial hippocampal sulcus. The margo denticulatus is a part of the dentate gyrus that has a toothed appearance [9]. It is separated from the subiculum by the superficial hippocampal sulcus and from the fimbria by the fimbriodentate sulcus. The gyrus dentatus and CA₄ are called area dentate [10]. It is important to recognize that the visible part of the gyrus dentatus has different names concerning the hippocampus but is, in fact, the same structure. It is called margo denticulatus in the body, the band of Giacomini in the uncus, and the fasciola cinerea in the tail.

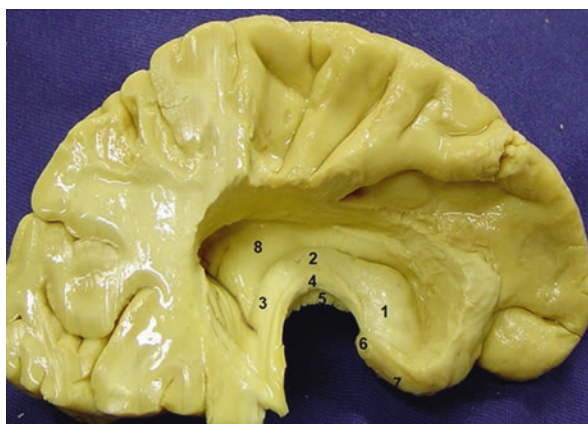
For didactic reasons, we think that the complex anatomy of the hippocampus can be described separately as head, body, and tail. Each of these regions is divided into intraventricular and extraventricular parts, as described by Duvernoy [7] (Fig. 9).

2.6 Hippocampal Head

In the intraventricular part, we identify three or four internal digitations sagittally oriented (digitations hippocampi). A vertical digitation that corresponds to the medial surface of the uncus sometimes can be identified. The digitations hippocampi are covered by part of the gyrus dentatus. The fimbria gives an alveus covering the hippocampal digitations at the junction of the body and head of the hippocampus. Another anatomical particularity is that there is no choroid plexus on the head of the hippocampus. The uncus recess is a prolongation of the temporal horn of the lateral ventricle anterior to the hippocampus that extends into the deeper portion of the uncus [9]. The basal and lateral nuclei of the amygdala “overhang” the hippocampal head and are almost joined together.

The extraventricular or uncus part of the anterior segment of the uncus is described below. The posterior segment of the uncus has an inferior and medial surface. The inferior surface is hidden in the uncus sulcus and can be visualized after resectioning the subjacent parahippocampal gyrus. It is divided into the band of Giacomini,

Fig. 9 Anatomical specimens of temporal pole, superior view, with an opened temporal horn to show mesial temporal structures: 1—head of the hippocampus; 2—body of the hippocampus; 3—tail of the hippocampus; 4—fimbria-fornix; 5—dentate gyrus; 6—tail of dentate gyrus; 7—uncus; 8—collateral eminence



external digitations, and inferior surface of the uncus apex. The band of Giacomini is the segment of the gyrus dentatus at the level of the hippocampal head. The external digitations are two or three small lobules anterior to the band of Giacomini that are the “inversion images” of the digitations hippocampi. The inferior surface of the uncus apex is separated from the band of Giacomini posteriorly by a small sulcus. The uncus apex is formed by CA₃ and CA₄ covered by the alveus and is the caudal end of the uncus. The medial surface is divided into the terminal segment of the band of Giacomini, which is localized on the upper lip of the uncus sulcus, the medial surface of the uncus apex, and the uncinatus gyrus, which joins with the gyrus ambiens and is anterior to the band of Giacomini (Fig. 9).

2.7 *Hippocampal Body*

The intraventricular part of the hippocampal body sits at the floor of the temporal horn of the lateral ventricle and is limited laterally by the collateral eminence (corresponds in the basal brain to the collateral sulcus) medially by the fimbria. It is covered by the choroid plexus, which is “attached” to a double layer, formed by ependyma and pia, that constitutes the tela choroidea. The tela choroidea is attached to the taenia of the tela choroidea. The inferior choroidal point, also known as velum terminale of Aebly, is a triangular lamella attached to the superior surface of the uncus where the taenia of the fimbria and stria terminalis unites. The term inferior choroidal point is not precise because there are no identified superior nor posterior choroidal points. The extraventricular part is formed by the gyrus dentatus, fimbria, and superficial hippocampal sulcus (Fig. 9).

2.8 *Hippocampal Tail*

The intraventricular part is limited medially and laterally by the fimbria and the collateral trigone, respectively. The choroidal plexus on this portion is larger (choroid glomus). Posteriorly, it reaches an intraventricular protrusion, the calcar avis. The hippocampal tail can be divided into initial, middle, and terminal segments in the extraventricular part. The initial segment is present as the margo denticulatus. The gyrus dentatus has many extensions penetrating deeply into the hippocampus. In the middle segment, the margo denticulatus becomes smooth and narrow, forming the fasciola cinerea. Still, in the middle segment, the fimbria ascends to join the crus fornices, and it is possible to identify the gyrus fasciolaris (CA₃ covered by alveus) separated from the fasciola cinerea by the sulcus dentofasciolaris. Contrary to the hippocampal body, CA₁ appears in the tail at the surface of the parahippocampal gyrus, sometimes producing the gyri of Anders Retzius [11]. The terminal segment of the hippocampal tail is formed by the subsplenial gyrus (Fig. 9).

2.9 Hippocampal Vascolarization and Vascular Relationships

According to their frequencies, the hippocampal arterial vasculature may be divided into six groups [12] (Fig. 10):

- *Group A:* Mixed arterial vasculature originating from the anterior choroidal artery (AChA), posterior cerebral artery (PCA), anterior inferotemporal artery (AIA), and splenic artery (SA). Present in 46.3% of hippocampi.
- *Group B:* Main origin at the temporal branches—main inferotemporal trunk (MIT), middle inferotemporal artery (MIA), posterior inferotemporal artery (PIA), AIA, or main branch of PCA. Present in 20.4% of hippocampi.
- *Group C:* AIA is the main branch of the hippocampus. Present in 14.8% of hippocampi.

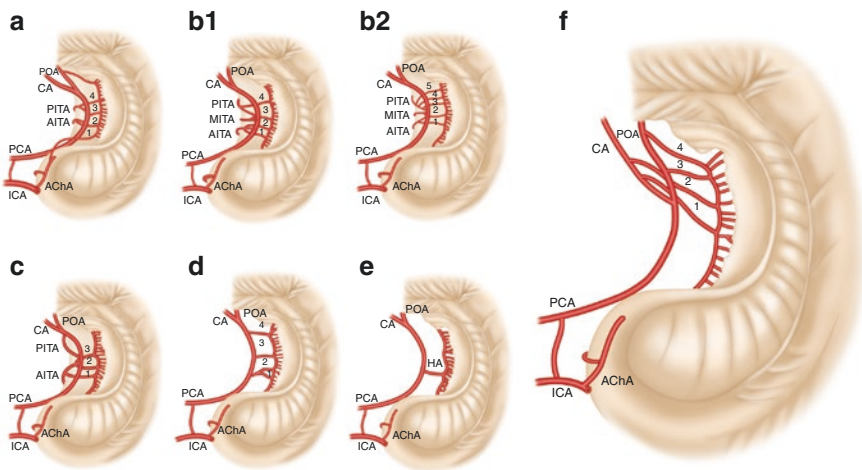


Fig. 10 Intra- and extraventricular view of the hippocampus vascularization groups. Hippocampal arteries present significant anatomical variations that have direct implications to surgical procedures such as amygdalohippampectomy. According to their origin, the hippocampal vascularization patterns can be categorized into six different groups. **(a)** Group A presents mixed irrigation, with the hippocampal arteries originating from the anterior choroidal, posterior cerebral, anterior inferior temporal, and splenic arteries. **(b1)** Group B presents hippocampal arteries originating from the inferior temporal branches and PCAs' main trunk. **(b2)** Also, Group B, but in a situation where the inferior temporal arteries arise from a common trunk. Arrowhead identifies a common inferior temporal artery. **(c)** Group C presents the anterior inferior temporal artery as the main feeder of the hippocampus. **(d)** Group D hippocampal arteries originate from the posterior cerebral arteries' main trunk. The hippocampal arteries are the largest contributors to the hippocampus blood supply in this group. **(e)** The trunk of the posterior cerebral artery originates from Uchimura's artery—a vessel that irrigates practically the whole hippocampus. **(f)** A new anatomical variation in which the hippocampal vessels arise exclusively from the POA, CA, and SA. CA calcarine artery, ICA internal carotid artery, PCA posterior cerebral artery, POA parieto-occipital artery, AITA anterior inferior temporal artery, MITA medial inferior temporal artery, PITA posterior inferior temporal artery, AChA anterior choroidal artery. 1, 2, 3, and 4: Hippocampal arteries. (Reprinted from Isolan et al. [12])

- *Group D*: HAs originating from the main branch of PCA. Present in 13% of hippocampi.
- *Group E*: A single hippocampal artery (HA) with the origin at the main branch of PCA. This single artery covered all of the structure and is named Uchimura's artery. Present in 3.7% of hippocampi.
- *Group F*: The hippocampal vessels arose exclusively from the parieto-occipital artery (POA), calcarine artery (CA), and splenic artery (SA). Present in 1.8% of hippocampi.

Regarding hippocampal vascularization, in 26.6% of hemispheres, one of the hippocampal vessels originates from the lateral posterior choroidal arteries and 36.6% from the splenic artery [13]. Regarding the variations, the most frequent pattern is characterized by mixed origins of the hippocampal arteries. This corresponds to Group A in the exhaustive studies carried out by Erdem et al. [13]. The hippocampal arterial supply was divided into five groups in this study according to the hippocampal supply origin. There is an average of 4.7 arteries per hemisphere supplying the hippocampus [13].

While the middle and posterior hippocampal arteries supply the hippocampal body and tail, the hippocampal head and uncus are supplied by the anterior hippocampal artery. An anastomosis can be present among these arteries [14]. In few cases, the arteries that supply the hippocampus can originate from a trunk: some important anatomical considerations are that these arteries vascularize the hippocampus by penetrating the dentate gyrus, the fimbrodentate sulcus, and the hippocampal sulcus. This, however, can be identified only if the fimbria is removed [13].

2.9.1 Anterior Choroidal Artery

The AChA has its origin in the posterior wall of the ICA. The AChA gives branches to the hippocampus in 31.5% of brain hemispheres, although some evidence suggests that it can be up to 50%. The HAs from the AChA have a similar conformation to the HAs from the PCA and follow the hippocampal sulcus in the uncus region. However, the arteries from the AChA supply mainly the head of the hippocampus [12].

2.9.2 Posterior Cerebral Artery

The PCA branches are divided into three groups: central (I), ventricular and choroid plexus (II), and cerebral branches (III). The ones related to hippocampal vascularization are the second and third. In the ventricular/choroidal plexus group, the posterolateral and posteromedial choroidal arteries supply the superior tela choroidea, choroid plexus of the lateral and third ventricle, thalamus, and internal region of the caudate nucleus. The cerebral group includes HAs, AIA, MIA, PIA, POA, CA, and SA. They supply the hemispheres' external occipital and ventral faces,

comprehending the inferotemporal, lateral occipitotemporal, medial occipitotemporal, and parahippocampal gyri. On the medial face, they supply the uncus, hippocampus, superior surface of the parahippocampal gyrus, and posterior areas of parietal and occipital lobes, including the precuneus and cuneus [12].

2.9.3 HA and Its Parent Vessels

The HA is one of PCA's first branches after its first segment (P1), as it arises directly from the PCA's main trunk, in up to 17.6% of the hemispheres. Although rare, it can also arise from the MIT (less than 1%). AIA, MIA, and PIA branch arteries to the hippocampus in, respectively, 57.4%, 0.5%, and 12.4% of the hemispheres.

The POA, which also arises from the PCA (P2 or P3 segments), may branch arteries to the hippocampus in up to 48% of hemispheres. The CA, medially and ventrally located to the POA, can emit hippocampal arteries in 31.5% of the hemispheres. Last, the SA (P3) has HA emerging in half of the hemispheres [12].

2.9.4 Vascular Arcades and Anastomoses

Anastomoses connecting the AChA or its branches to the PCA, POA, and CA (or their branches) can be seen in almost half of the brain hemispheres. These anastomoses connect the uncus branches of the AChA to the HAs of the cited vessels. In most cases, the anastomoses have an arcuate conformation.

At the level of the choroid plexus of the lateral ventricle's temporal horn, anastomoses have been identified connecting the AChA or its branches to posterior choroïdal arteries (PChA) descending from the PCA. Both lateral PChA branches and distal AChA branches provide blood supply to important structures, such as the lateral geniculate nucleus, and therefore, it is essential to recognize these anastomoses to avoid visual field deficits [12].

2.10 Amygdala

The amygdala can be divided into "temporal or principal amygdala" and "extratemporal or extended amygdala." The first one can be subdivided into basolateral, corticomедial, and central groups and can be described as located into the uncus. The temporal amygdala blends with the globus pallidus superiorly, forming the anterior part of the roof of the temporal horn. Its inferior portion constitutes the anterior wall of the temporal horn. Therefore, the amygdala is closely related to the temporal horn, limiting this structure by designing its anterior wall and the major part of its anterior roof. Anteriorly, the amygdala merges with the rest of the uncus through the semilunar gyrus and relates to the entorhinal area anteroinferiorly [15].

The amygdala represents a bottom line for the limbic system and is especially implicated in fear and aversive responses. Some evidence also points to at least some involvement with positive emotions, such as a minor role in reward processing [16]. Although these functions might be harmed with the amygdectomy, it is worth noting that not much impairment is expected from the removal of the amygdala in mesial temporal epilepsy surgeries once this region is presumably already damaged in such situations [17].

2.11 Choroidal Fissure

The choroidal fissure is a C-shaped cleft between the thalamus and the fornix localized from the foramen of Monro to the temporal horn of the lateral ventricle. It gives attachment to the choroid plexus in the lateral ventricle. This plexus, filling the choroidal fissure, is also C-shaped, revolving around the thalamus superiorly, posteriorly, and inferiorly. In the temporal horn, the choroidal fissure is located between the stria terminalis of the thalamus, superomedially, and the fimbria, inferolaterally, forming the inferior choroidal point (its inferior termination) next to the lateral geniculate body and behind the uncus.

The choroidal fissure might be didactically divided into three segments: body, atrial, and temporal. The body is located in the body of the third ventricle, precisely between the body of the fornix and the superior surface of the thalamus. The atrial part is situated amid the crus fornices and the pulvinar region of the thalamus. Finally, the temporal part is located between the fimbria of the fornix and the inferolateral thalamus, medially to the temporal horn. The choroidal fissure is a natural corridor and the best anatomic surgical landmark used for resection en bloc of the mesial temporal structures.

It takes around 8 weeks of embryonic progress for the epithelial roof of the third ventricle to invaginate itself medially and create the choroidal fissure. The fact that no nervous tissue is formed between the ependyma and the pia mater at this event causes an interesting anatomic singularity for the neurosurgical approach. It allows this area to become a proper access path to several structures with diminished risk for injuries and neurologic deficits [18, 19].

2.12 Vascular Relationships

Although there is a great number of arteries and branches that are important concerning the amygdalohippocampectomy, for a didactical purpose, we will briefly discuss the internal carotid artery, posterior communicating artery, anterior choroidal artery, posterior cerebral artery, and middle cerebral artery.

The ICA has a supraclinoid segment that enters the intradural space on the carotid cistern on the medial side of the anterior clinoid process below the optic nerve and runs superiorly dividing into ACA and MCA. The posterior communicating artery emerges from the inferolateral wall of the ICA and runs posteromedially, passing close or even adherent to the dura of the posterior clinoid process to pierce the interpeduncular cistern. Here, it joins to the posterior cerebral artery, between P1 and P2 segments.

The posterior cerebral artery arises as to the terminal branches of the basilar arteries in the interpeduncular cistern. The P1 segment is not related to the uncus. The thalamoperforating arteries are the main branches of P1. The P2 segment running into the crural cistern is related to the posteromedial segment of the uncus. The medial posterior choroidal, the short and long circumflex, and the hippocampal arteries arise from this P2 segment. The lateral posterior choroidal artery arises from the P2 segment that runs into the ambient cistern and enters the temporal horn via choroidal fissure. The P2 segment bifurcates in inferolateral and superomedial trunks. The inferolateral trunk gives rise to the inferotemporal branches (anteroinferior, inferomedial, inferoposterior, and inferotemporo-occipital). After loops into the ambient cistern, the superomedial trunk gives rise to the calcarine and parieto-occipital arteries.

The anterior choroidal artery arises in most cases from the posterolateral wall of the internal carotid artery between the posterior communicating artery (PComA) and the carotid bifurcation. There are branches from the inferomedial wall of the ICA between PComA and AChA that supply the optic tract and posterior perforated substance.

The basal vein of Rosenthal is the main venous channel that drains the mesial temporal region. The basal vein originates below the anterior perforated substance by the union of the deep middle cerebral, inferior striate, olfactory, fronto-orbital, and deep middle cerebral veins. It runs posteriorly under the optic tract and medially and inferiorly to the anterior portion of the crus cerebri. This point corresponds to the most inferior and medial part in its course before its termination in the vein of Galen. The hippocampal veins drain to the inferior ventricular vein and then to the basal vein.

2.13 Optic Radiation

The most important relationships for neurosurgeons correlate with the anatomical surface of the temporal lobe and the optic radiations. Axons of the neurons in the lateral geniculate nucleus project to the visual cortex in the occipital lobe via the geniculocalcarine tract (optic radiation). The anterior inferior fibers of the optic radiation curve toward the pole of the temporal lobe before making a sharp curve to return posterolaterally. This curve is called “temporal knee” [20], “temporal loop”

[21], or “Meyer-Archambault loop” [22]. The essential knowledge is related to the distance of the temporal tip and the most anterior fibers of Meyer’s loop. According to Yasargil [3], this measurement cannot be precisely addressed with the fiber microdissection technique due to the dense network of fibers, especially in the area of the sagittal stratum, which would destroy one fiber tract in the identification of the other and vice versa. However, this subject is controversial.

In our fiber dissections, the sequential steps followed those addressed by Yasargil [3]. We began taking the cortex out, which exposed the arcuate fibers. The arcuate fibers interconnect adjacent cortex areas and are U-shaped when they have to circumvent the bottom of a sulcus between adjacent gyri. Dissecting these most superficial layers of white matter underlying the cortex of the temporal lobe and occipital lobe and the area around the Sylvian fissure, the superior fasciculus longitudinalis was identified. After this fascicle is peeled away, part of the sagittal stratum is identified, although it is difficult to disentangle from the external sagittal stratum [4]. The sagittal stratum is formed by the occipitofrontal fasciculus and the posterior thalamic peduncle, but it is difficult to individualize the different tracts. The sagittal stratum passes from the temporal lobe toward the occipital lobe, and fibers of the optical radiation are included here. The “occipital-temporal projection system” is a chain of short cortico-cortical fibers running external to the sagittal stratum next to the optic radiation that interconnects the anterior temporal cortex to the occipital pole [23]. The cortex of the insula was removed, and extreme capsule was identified. The extreme capsule is a thin fiber system that connects the frontal and temporal opercula with the insula. After this subsequent external-to-internal dissection, the following structures were identified: claustrum, external capsule, putamen, globus pallidus, and internal capsule. The optic radiation constitutes part of the posterior thalamic peduncle, which is part of the internal capsule. The frontal and temporal lobes are connected more anteriorly by the uncinate fascicle, which overlies the amygdala. Its fibers gather under the cortex of the limen insulae, where they form a very compact bundle. The inferior fronto-occipital fasciculus (IFOF) occupies the extreme and external capsules during part of its course. This fascicle carries fibers between the midportion of the superior temporal gyrus (auditory association cortex) and the dorsolateral and mesial prefrontal cortex, between the prefrontal cortex and midportion of the inferior temporal cortex (visual association cortex) and multimodal cortex of the superior temporal sulcus, and between the dorsolateral prefrontal cortex and the parahippocampal area. It is associated with the uncinate fasciculus at the limen insulae.

Part of the optic radiations from the lateral wall of the temporal horn become thicker more posteriorly due to the inclusion of the fibers of the inferior fronto-occipital fasciculus to become the sagittal stratum. The inferior end of the optic radiation does not go inferior to the inferior temporal sulcus. The optic radiation can be divided into three groups of the same size. One is called the posterior bundle and is part of the sagittal stratum. These fibers do not do any anterior curve. The other is the central bundle that makes a partial anterior curve and courses within the sagittal stratum posteriorly. The other is the anterior bundle, also known as Meyer’s loop, which courses around the lateral half of the tip of the temporal horn before entering

into the sagittal stratum. In the posterior end of the temporal lobe, these fibers turn and become inferior to the occipital horn to approach the inferior bank of the calcarine fissure.

In our dissections, we noted that the full extension of the lateral and superior wall of the temporal horn was covered by optic radiation, and even the lateral half of the tip of the temporal horn, reaching the anterior edge of uncal recess and extending a few millimeters (range 2 mm) anterior to the tip of the temporal horn [24]. The inferior and medial walls of the temporal horn are free of optic radiation, except at the level of the lateral geniculate body.

At coronal sights, the temporal lobe seems to be connected to the basal forebrain through a peduncle resembling a tree's roots. This structure is widely called the temporal stem. Although the terminology is largely used, the temporal stem is not a well-established concept. It ranges from being only the fibers that pass between the limen insula and the temporal horn to all the fibers that pass under the inferior limiting insular sulcus. At its larger definition, the brain stem comprises the anterior commissure, the uncinate fasciculus, the inferior fronto-occipital fasciculus, Meyer's loop of the optic radiations, and inferior thalamic fibers, measuring up to 8.2 mm [25, 26].

Access to the amygdala and hippocampus through the temporal horn is crucial at the transsylvian approach to the medial temporal lobe. Thereby, the neurosurgical value of knowing the temporal stem anatomy is related to this method, once the gateway through the structures described above is generally directed through the temporal stem [25, 26] (Figs. 11, 12, 13, 14, 15, 16, and 17).

2.14 Inferior Fronto-Occipital Fasciculus

The inferior fronto-occipital fasciculus (IFOF) is a large association bundle of fibers (white matter) that, as the name suggests, connects the frontal and occipital lobes. It runs through the insular lower portions within the extreme and external capsules. Although it runs above and posteriorly the uncinate fasciculus, there is no defined limit between them in the white matter. It also has a close relationship with the optic radiation, running parallel and above them [27]. Its fibers connect the frontal gyri; run under the superior, anterior, and inferior insular limiting sulci; and reach temporal, parietal, and occipital regions [28].

Based on the intraoperative neurophysiological subcortical stimulation during surgery in awake patients, it is associated with the IFOF contributions to awareness; elaboration of visual information for motor planning, reading, and attention; as well as a role in semantic components of language. Therefore, transinsular surgical approaches must be made with caution. A deep transinsular approach, mostly at the dominant hemisphere (but maybe even in the non-dominant side), can damage the IFOF and may lead to language deficits [28] (Figs. 11, 12, 13, 14, 15, 16, and 17).

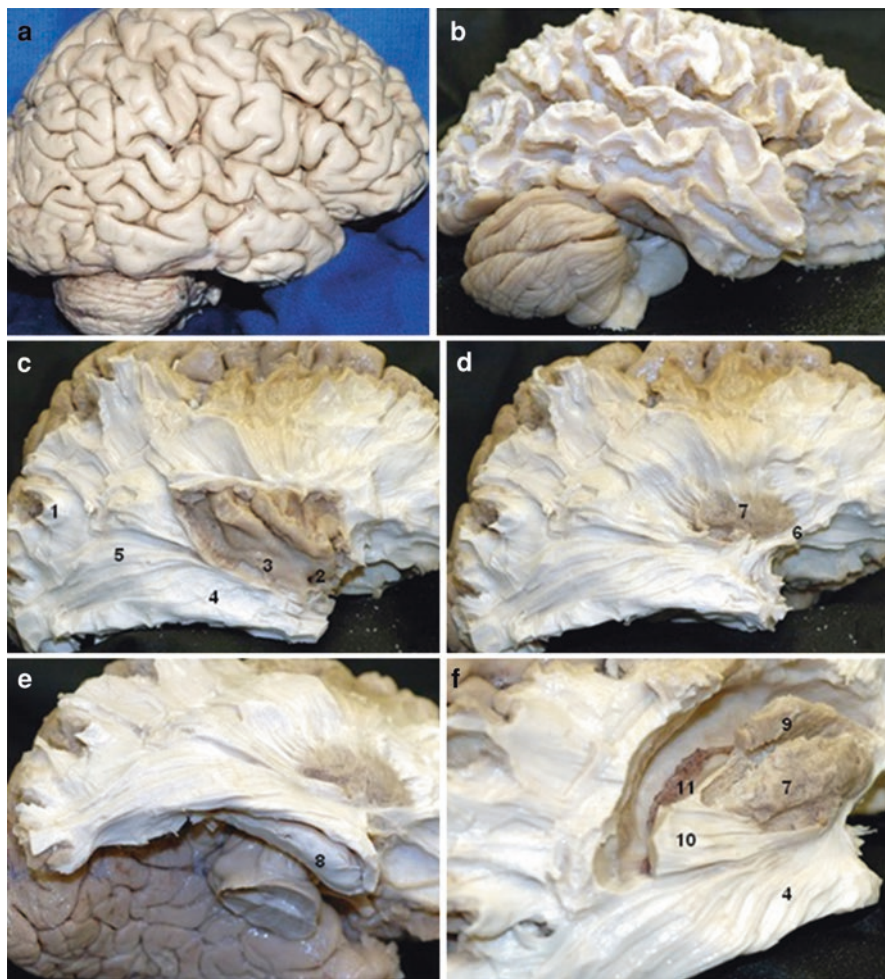


Fig. 11 Lateral view of right-sided brain hemisphere showing step-by-step white fiber dissection. (a) Lateral view of the right side of the brain; (b) grey matter removed, exposing the U-fibers in the white matter; (c) further white matter dissection, exposing the Meyer's loop, sagittal stratum, and insular grey matter; (d) grey matter of the insula removed; (e) inferolateral view of the dissected right-side brain, showing the inferior view of the hippocampus; after dissection of the central core, exposing the basal nuclei and its relation with the temporal horn of the lateral ventricle; (f) superior and lateral view of the Meyer's loop and optic radiation. 1—U-fibers; 2—Sylvian vallecule; 3—insular cortex; 4—Meyer's loop; 5—sagittal stratum; 6—uncinate fasciculus; 7—putamen; 8—hippocampus; 9—caudate nuclei; 10—inferior fronto-occipital fasciculus; 11—choroid plexus

Fig. 12 Closer look to a latero-inferior view of white fiber dissection, showing the hippocampus and its relation to Meyer’s loop

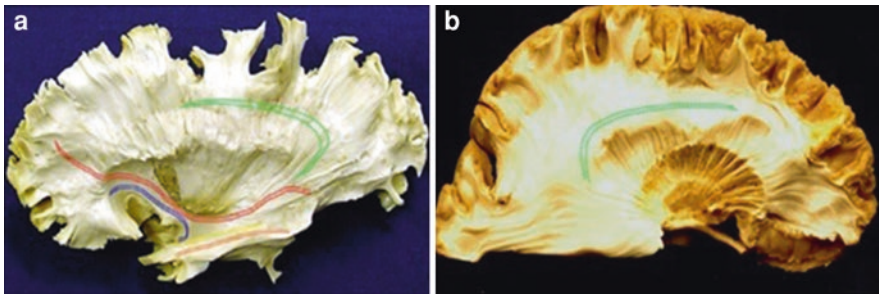


Fig. 13 White fiber dissection and schematics of the fasciculi. (a) Long association fiber representation. Arcuate fasciculus (green); inferior fronto-occipital fasciculus (red); middle longitudinal fasciculus (yellow); inferior longitudinal fasciculus (orange). (b) Long association fiber representation. Arcuate fasciculus (green)

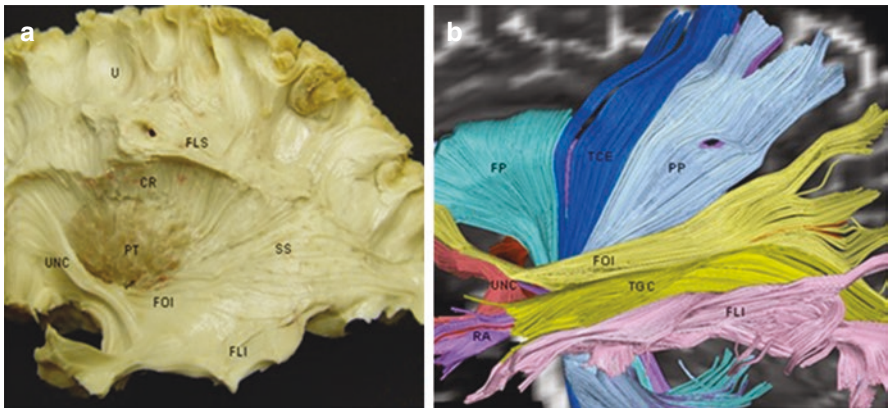


Fig. 14 (a) White fiber dissection showing association fibers and (b) white fiber schematics based on tractography. *UNC* uncinate fasciculus, *PT* putamen, *FOI* inferior fronto-occipital fasciculus, *FLS* superior longitudinal fasciculus, *SS* sagittal striatum, *CR* corona radiata, *FLI* inferior longitudinal fasciculus, *U* U-fibers, *FP* frontopontine fibers, *TCE* corticospinal tract, *PP* parietopontine fibers

Fig. 15 Parasagittal brain section through the hippocampus: 1—insular cortex; 2—caudal part of the hippocampus; 3—collateral sulcus; 4—alveus and fimbria-fornix; 5—temporal horn of lateral ventricle; 6—rostral part of the hippocampus; 7—temporal horn of lateral ventricle; 8—amygdala; 9—tail of caudate nucleus; 10—putamen

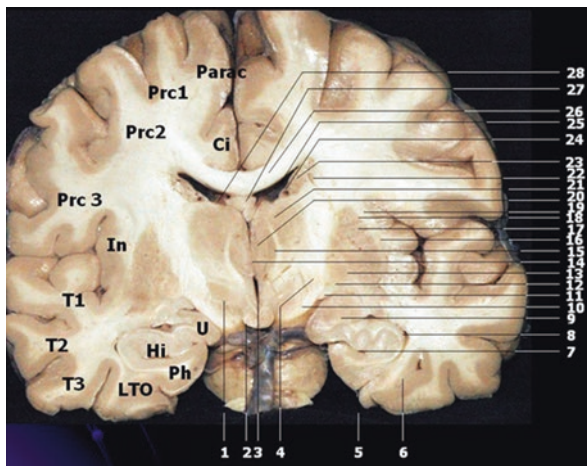
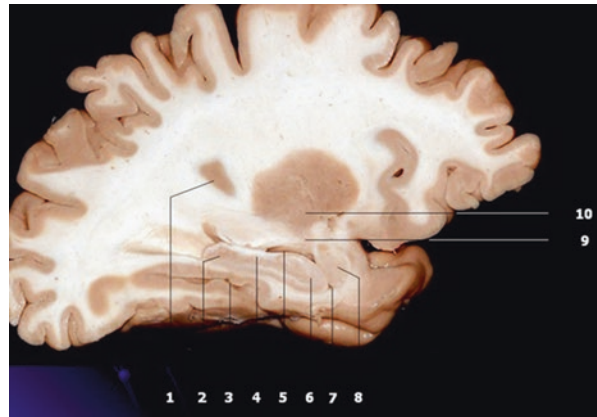


Fig. 16 In a coronal section, we can see that there are no basal ganglia in the superior limiting insular sulcus before the internal capsule. It is easy to damage the corona radiata and disrupt important descending (motor) and ascending (sensitive) fibers. We can also see that the inferior limiting insular sulcus is directly related to the temporal stem. There are several white matter fasciculi in the temporal stem, which could cause different deficits if damaged: 1—lenticular fasciculus; 2—mammillary bodies; 3—third ventricle; 4—posterior limb of internal capsule; 5—collateral sulcus; 6—occipitotemporal sulcus; 7—hippocampal fissure; 8—temporal horn of lateral ventricle; 9—amygdala; 10—cerebral peduncle; 11—optic tract; 12—medial globus pallidus; 13—internal medullary lamina (thalamus); 14—interthalamic adhesion; 15—mammillothalamic tract; 16—claustrum; 17—putamen; 18—external capsule; 19—extreme capsule; 20—anterior nucleus of thalamus; 21—ventral anterior nucleus of thalamus; 22—caudatolenticular transcapsular grey stria; 23—caudate nucleus; 24—stria terminalis; 25—body of lateral ventricle; 26—corpus callosum; 27—fornix; 28—choroid plexus; U—uncus; Hi—hippocampus; Ph—parahippocampus; LTO—lateral occipito-temporal gyrus; T1—superior temporal gyrus; T2—middle temporal gyrus; T3—inferior temporal gyrus; In—insula; Prc 1—superior peduncle of precentral gyrus; Prc2—middle peduncle of precentral gyrus; Prc3—inferior peduncle of precentral gyrus; Parac—paracentral gyrus; Ci—cingulate gyrus

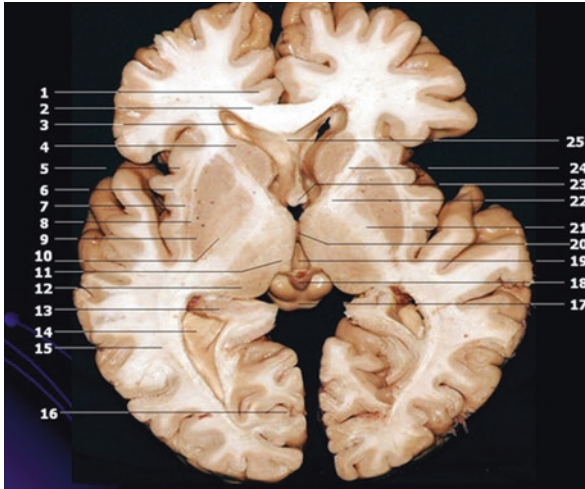


Fig. 17 Axial brain section through the lentiform nuclei, emphasizing all white matter layers from the insular cortex to the internal capsule: 1—cingulate gyrus; 2—genu of the corpus callosum; 3—frontal horn of lateral ventricle; 4—head of caudate nucleus; 5—insular cortex; 6—extreme capsule; 7—claustrum; 8—external capsule; 9—putamen; 10—globus pallidus; 11—thalamus; 12—pulvinar nucleus (thalamus); 13—choroid plexus; 14—occipital horn of lateral ventricle; 15—tapetum (corpus callosum); 16—calcarine sulcus; 17—quadrigeminal plate; 18—pineal gland; 19—third ventricle; 20—interthalamic adhesion; 21—posterior limb of the internal capsule; 22—genu of the internal capsule; 23—anterior column of fornix; 24—anterior limb of the internal capsule; 25—septum pellucidum

2.15 *Uncinate Fasciculus*

The uncinate fasciculus (UF), named after its “hook” shape, is a bundle of association fibers that connects the anterior and medial portions of the temporal lobe to the orbital portion and the pole of the frontal lobe. It lies under the cortex of the limen insulae, anteroinferiorly to the IFOF and the optic radiation (Meyer’s loop) [27].

It is hypothesized that the UF is just part of a semantic network that involves the UF, the inferior longitudinal fasciculus (ILF), and the IFOF, with the UF being the link between the occipitotemporal pathway of the ILF and the frontal lobe. As it has a close relation to the IFOF, it is also associated with semantic components of language, although to a lesser extent. Some studies also attribute to the UF some naming functions (objects or actions) and face recognition, although studies show mild to no speech deficits after UF resection (tumor or epilepsy surgery). Another important factor that should be considered is that slow-growing lesions, such as a low-grade glioma, induce neuroplasticity, allowing redistribution of language functions to healthier sites [29] (Figs. 11, 12, 13, 14, 15, 16, and 17).

2.16 *Temporal Stem*

Although not precisely defined, the temporal stem is a widely used term referring to the fibers passing underneath the inferior limiting insular sulcus. The name “temporal stem” is derived from the appearance, in the coronal plane, that there is a “peduncle” of white fibers, which pass deep through the anterior aspect of the insula, connecting the temporal lobe to the central core, and it may look like the “roots of a tree.” Its concept ranges from just the fiber bundles passing between the limen insula and the anterior end of the temporal horn to all the fibers passing beneath the length of the inferior limiting insular sulcus (ILS) [26, 28].

In its larger definition, the temporal stem has been divided into two components, anteromedial and posterolateral, the first being formed by the ventral amygdalofugal fibers, UF, anterior aspects of the IFOF, and anterior commissure and superior extension of the amygdala toward the globus pallidus, and the latter by the fibers that pass underneath the insular limiting sulcus between the tip of the temporal horn and lateral geniculate body-posterior aspects of IFOF and anterior commissure, and optic radiation fibers [26, 28] (Figs. 11, 12, 13, 14, 15, 16, and 17).

2.17 *Language in the Temporal Lobe*

The advance from a localizationist paradigm to a hodotopical model (network of cortical areas and their connecting pathways) has been largely having taken place with modern techniques that allow scientists to study language function in vivo, such as direct electrical stimulation (DES) in awake craniotomies, diffusion tensor imaging and fiber tractography, functional MRI, magnetoencephalography, and navigated transcranial magnetic stimulation. These techniques provide a more accurate insight into the actual organization and functioning of the brain, while traditional models, built on evidence from patients with cortical lesions, do not explain the multiples aspects of speech function and its connections with other areas [30].

Anatomical and tractographical studies have facilitated the identification of white matter tracts involved in language functions. Intraoperative DES provides a unique opportunity to discover the functional roles of cortical hubs and subcortical pathways [31].

Dysarthria is related to the lateral precentral and the postcentral gyri on both sides of the brain, suggesting that the sensory system modulates the articulatory process. Speech articulation is presumed to be a bilateral process within the face motor cortices [30, 31]. In anomia, speech is partially preserved, but nouns are difficult to retrieve. The epicenter of this function seems to be located in the posterior superior temporal gyrus and the inferior parietal lobule of the dominant hemisphere, corresponding to the “classical” Wernicke’s area. However, other areas may also be involved (inferior precentral gyrus, close to the lateral sulcus and middle frontal and the precentral gyri, which is also the junction between the dorsal and ventral premotor cortices) [30, 31].

Semantic and phonological processes are widely distributed throughout the cortex in the dominant hemisphere. Semantics is associated with the junction of the posterior superior temporal gyrus and the supramarginal gyrus, pars triangularis, pars opercularis, and dorsal premotor cortex. Phonology is associated with the middle superior temporal gyrus, the pars opercularis, and the junction of the dorsal and ventral premotor cortices. The localization of semantic and phonological processes in the pars triangularis and the pars opercularis suggests that the classical Broca's area could be involved in higher order tuning of language [31].

The arcuate fascicle (AF), deep portion of the superior longitudinal fascicle that connects the posterosuperior temporal cortex and the inferior parietal cortex to areas in the frontal lobe, is associated with several language dysfunctions such as Broca's aphasia, alexia, agraphia, conduction aphasia, reduced comprehension, anomia, dyslexia, Wernicke's aphasia, and transcortical sensory aphasia. Lesions in the uncinate and inferior longitudinal fasciculi are associated with semantic dementia [31].

2.17.1 Language Input

The first stage in the process of understanding language involves visual, auditory, or somatosensory input. Visual perception is the first stage of a language process elicited by visual input. The visual occipital cortex is connected to the fusiform gyrus (both visual object form area (VOFA) and visual word form area (VWFA)) by the inferior longitudinal fascicle, and stimulation of this pathway triggers visual paraphasia.

Subcortical DES of the occipitotemporal white matter tracts on the dominant hemisphere induced different lower and upper fiber symptoms. In the same patients, stimulation of lower fibers induced alexia, while stimulating the upper fibers induced anomia. Therefore, words and objects seem to be recognized by two distinct and parallel pathways originating from the visual occipital cortex.

Auditory input from the thalamus is processed in multiple locations, such as the posterosuperior temporal areas and the supramarginal, angular, posterior middle temporal, superior, and middle occipital gyri. These locations are interconnected by U-fibers [30, 32].

Somatosensory input information from the thalamus is processed in the superior parietal lobule, the precuneus, the superior cingulate cortex, the SMA, the primary motor cortex, the prefrontal cortex, the middle frontal gyrus, and the orbitofrontal areas, which are also interconnected by U-fibers [30, 32].

2.17.2 Semantic Versus Phonological Pathways

Visual and auditory language processes seem to branch into two main pathways, ventral semantic and dorsal phonological, which interact and work in parallel. In auditory language processing, the ventral stream could be involved in mapping sound to meaning, and the dorsal stream in mapping sound to articulation. This dual

model was built for visual language processing based on DES-induced separation between phonemic and semantic processes, demonstrating that these processes do not occur serially but in parallel [30].

2.17.3 Ventral Semantic Stream

The IFOF subserves the direct pathway of the ventral semantic stream. The IFOF connects the posterior occipital lobe and the VOFA to frontal areas such as the dorsolateral prefrontal cortex and the pars orbitalis. DES of the IFOF resulted in semantic paraphasia [26, 30].

In addition to the direct pathway, there is an indirect pathway with a relay in the temporal pole. This indirect ventral stream is subserved by the anterior part of the inferior longitudinal fascicle, which connects the VOFA to the temporal pole. From the temporal pole, the information is relayed to the pars orbitalis by the UF. This sub-network can be bypassed to the direct pathway (IFOF) and functionally compensated, explaining the lack of speech deficits following UF damage.

Another sub-network, the middle longitudinal fasciculus, could be involved in the ventral semantic stream. This pathway connects the angular gyrus to the superior temporal gyrus. However, this fasciculus has not elicited naming disorders, so its specific functional role remains unknown [30].

2.17.4 Dorsal Phonological Stream

The dorsal pathway is subserved by the superior longitudinal fascicle and can be divided into two components. The deeper one is the AF, which runs from the posterior section of the middle and inferior temporal gyri, arches around the insula, and moves toward the ventral premotor cortex and the pars opercularis.

In several studies, phonemic paraphasia was observed after DES of white matter around the superior and posterior parts of the superior insular sulcus. The VOFA, involved in both phonological and semantic processes, is the posterior cortical origin of the dorsal pathway.

Stimulation of the AF induces conduction aphasia without semantic disorders. Conduction aphasia is a phonemic paraphasia combined with repetition disorders. These findings support the role of the AF in phonological processing [30, 32].

The more superficial component of the dorsal stream is subserved by the anterior part of the superior longitudinal fascicle, as anarthria was observed after DES [32]. This bundle connects the posterior part of the superior temporal gyrus and the supramarginal gyrus to the ventral premotor cortex. Therefore, this system integrates somatosensory and auditory information with phonological-phonemic information translated into articulatory motor programs. This loop is also used during word repetition [30, 32].

2.18 *Brain Hodotopy*

Brain hodotopy is an oppositional concept to the long-established topological and fixed vision of brain organization. Hodotopy sees the nervous system as a dynamic entity with an interconnected and ever-changing network, contrasting with the localizationist view. It has been applied in neuro-oncological surgeries for presurgical planning, aiming to preserve noble regions of the brain, admitting and foreseeing its dynamic nature [33, 34]. Nevertheless, hodotopy is still disregarded in epilepsy surgeries [33]. This is an inquisitive situation considering that the hodotopical concept is especially fit to epilepsy cases, once the disturbance present in such situations seems to be a particularly good source for functional reorganization [35]. In order to avoid potential functional deficits, as mentioned above, we hope that hodotopy will be better explored for epilepsy surgery soon.

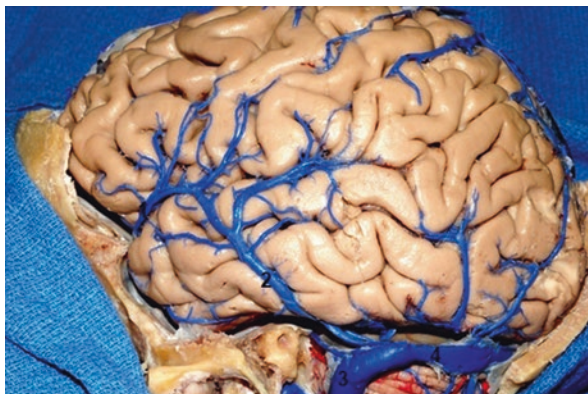
2.19 *Sylvian Cistern*

The lateral sulcus (Sylvian fissure), easily observable from a lateral view, is the largest sulcus of the brain, which makes it a trendy access in neurosurgery. It sits over the insula and is designed to wrap the frontal, parietal, and temporal opercula. The Sylvian fissure transitions between the basal cisterns and the subarachnoid space over the convexities [36]. Concerning the Sylvian fissure, the proximal aspect of the Sylvian cistern is at the level of the origin of the middle cerebral artery from the internal carotid artery. It narrows distally as the frontal and temporal lobes approach each other over a length of 15–20 mm. The relation between the frontal and temporal lobe on the Sylvian fissure is inconstant, difficult for dissection. The arachnoid membranes in the lateral sulcus can be transparent and fragile or thickened and tough. Professor Yasargil divides this relation into four categories, in crescent order of difficulty at dissection. The cistern is large over the insula. The structures sitting in the Sylvian cistern are the superficial and deep Sylvian veins, the middle cerebral artery, and the origin of its branches [36–39].

2.20 *Superficial Sylvian Veins*

The superficial Sylvian veins are one or more large veins that are generally related to the temporal part of the lateral sulcus. There is much variation in the number and course of the superior and deep Sylvian veins. Generally, they drain into the sphenoparietal sinus and, less frequently, into the cavernous sinus. Although there is a rich collateral system in these veins, the purpose of the neurosurgeon is to preserve all of them, once it is not possible to know what vein sacrifice will lead to venous infarction and neurological deficit [37, 39] (Fig. 18).

Fig. 18 Lateral view of left-sided brain hemisphere showing superficial temporal drainage system: 1—superficial middle cerebral vein (superficial Sylvian vein); 2—inferior anastomotic vein (vein of Labbe); 3—sigmoid sinus; 4—transverse sinus



2.21 Middle Cerebral Artery

The middle cerebral artery (MCA) originates from the internal carotid artery. Its first segment, M1, ranges from its origin to the bifurcation and gives two groups of branches, the temporal vessels and the perforating vessels. The temporal vessels or superior lateral group are, ordered proximal to distal, the uncal artery (this artery originates from ICA in 70% of the cases), polar temporal artery, and anterior temporal artery. The M1 segment divides in the M2 segment at the limen insulae. The M2 segment is composed of superior and inferior trunks.

There are many variations in the vascularization pattern of the temporal lobe by these arteries, but one very important variation is the false bifurcation of the MCA, which is a large branch from the lateral wall of the proximal M1 segment that gives the impression of a true early bifurcation. The perforating vessels, the inferior medial group, or “lenticulostriate vessels” are 2–15 [36]. The most common pattern is all the lenticulostriate arteries arising from one single large artery. The course of the M1 segment is not only straight but also C- or S-shaped. The true bifurcation of the MCA always occurs at the high point of the limen insulae. The fenestration of the proximal part of the M1 occurs in 0.1–0.3% [40]. An accessory MCA can be present in 0.5% of cases and originates from the proximal or distal A1 segment [40]. When large branches arise from either the superior or the inferior trunks close to the bifurcation, an impression of a “pseudo-trifurcation” or “pseudo-tetrafurcation” may be given [41]. However, true trifurcation, tetrafurcation, or even pentafurcation is present only in few cases [36] (Fig. 19).

Fig. 19 Pseudo-tetrafurcation of the middle cerebral artery



3 Temporal Surgery for Epilepsy

Resective surgery to treat epilepsy was first described by Horsley in 1886 [42]. Since then, with the advent of electroencephalography and electrocorticography, temporal surgery has been continually improving. In early practice, hippocampus preservation was thought to be mandatory to avoid memory deficits, but it has been proved that seizure control cannot be achieved without mesial temporal structure resection [43]. The goal of treatment is to reach a state of “seizure freedom,” as it improves the patient’s quality of life (education, employment, social life).

Several techniques have been proposed for resection of temporal structures to be less resective and more efficient, reducing the chance of neurological deficits. However, it is not well established which technique (selective or not) has better seizure control and lower deficit risk (Fig. 20).

The selective amygdalohippocampectomy and the anterior temporal lobectomy are the two techniques used to treat mesial temporal lobe epilepsy. There are two different anatomical routes to perform the selective amygdalohippocampectomy, the transsylvian and the transcortical approaches. Our dissections and results were exposed in the transsylvian way because this route is more anatomical, although more skills are required due to work at the Sylvian fissure.

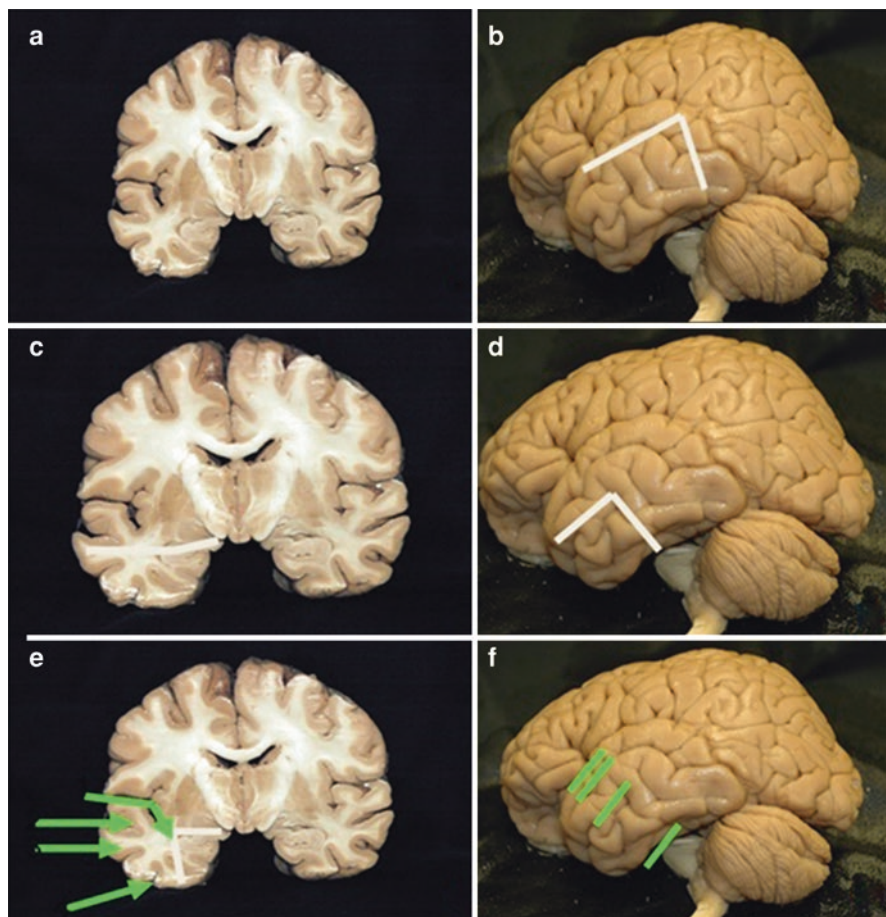


Fig. 20 Sagittal and coronal views of anatomical specimens of the brain, with schematics of temporal approach in epilepsy surgery. (a, b) show anterior temporal lobectomy. (c, d) show Spencer's technique. (e, f) show multiple possibilities of selective amygdalohippocampectomy (transylvian, transtemporal, or subtemporal)

3.1 *Neurological Deficits Following Temporal Epilepsy Surgery*

Visual field deficits (VFDs) are a major debate in epilepsy surgery, a controversy especially intense at transylvian approaches. Around 36% of the patients subjected to the procedure have some VFDs, but this statistic can be shifted to much higher values depending on the study and approach selected. Although a fair amount of these patients is not aware of their deficits, the loss can lead to important problems, such as driver's license acquisition [44, 45].

Some experts argue that damage to the branches that supply the optic radiations and the lateral geniculate body, mostly coming from the anterior choroidal artery, is the main source of VFDs after epilepsy surgeries. However, there is evidence supporting otherwise, mainly experience with surgeries for parkinsonism. In such situations, the obliteration of the very anterior choroidal artery does not seem to lead to VFDs [44].

Presently, the predominant view is aligned with the idea of direct damage to the optic radiations. When approaching the temporal horn through the floor of the Sylvian fissure, the anterior bundle of optic radiations (Meyer's loop) can be impaired [24]. The exact location of this fiber is not consensual. Over time, it has been estimated to be between 20 and 60 mm behind the temporal pole [44]. Through modern techniques, different studies found different but similar values, ranging between 22 and 43 mm. Anyway, Meyer's loop position certainly admits a spectrum of anatomic varieties [45–47].

Choi et al. [24] proposed a triangular area where the temporal horn could be approached with diminished risk for optic radiations. This area is situated between Meyer's loop and the optic tract. The base of the triangle would be near the amygdala, at the level of the limen insula. The anterior edge of the lateral geniculate body would be at the apex of the triangular area. Thereby, a transsylvian incision should be made adjacent to 5 mm of the inferior limiting sulcus. Another proposed option is the use of fiber tracking to predict optic radiation damage in surgeries. Some studies demonstrated the usefulness of diffusion tensor imaging techniques for this purpose. Nevertheless, this is not a real-time procedure and does not consider brain shift [45, 47–49].

Another structure worth mentioning is the uncinate fasciculus, which connects orbitofrontal to temporopolar areas and presumably supports mnemonic associations such as face and object recognition [50]. At transcortical SAH, incisions after the limen insula posterior limits fatally injure this bundle. This might be related to the memory deficits described after the procedure. Also related to the limen insula, the inferior occipitofrontal fasciculus can be impaired in incisions to the inferior limiting sulcus, which might produce paraphrasing episodes [51].

3.2 Standard Temporal Lobectomy

The standard temporal lobectomy (anterior temporal lobectomy) consists of resection of mesial and lateral temporal structures, which can be done en bloc or separately. The resection of lateral structures allows the visualization and en bloc resection of the hippocampus.

The patient lies in a supine position with contralateral head rotation. Pterional craniotomy is followed by a durotomy that exposes the Sylvian fissure and the temporal lobe. The corticectomy starts in the lateral temporal surface, 4–5.5 cm

posterior to the temporal tip (if dominant hemisphere, the incision must be closer). A slight anterior deviation in the T1 gyrus may be useful to avoid Heschl's gyrus (primary auditory cortex). Upon reaching the upper temporal border, a subpial dissection is performed through the medial surface to preserve the MCA and its branches. The insula is then exposed. The resection is expanded from the lateral gyri through the fusiform gyrus up to the collateral sulcus, and the temporal horn of the lateral ventricle is opened. From now, the head of the hippocampus can be seen. The temporal stem can now be resected in the inferior insular limiting sulcus. The temporal neocortex (lateral portion) can be removed by sectioning the leptomeninges lateral to the temporal horn. Further mesial resection can be done if an en bloc anterior temporal lobectomy is the goal. Care must be taken during resection of mesial structures, not to damage the posterior cerebral artery, the basal vein of Rosenthal, the third cranial nerve, and the midbrain and not to go medially or superiorly to the globus pallidus. The entorhinal cortex is resected to the anterior portion of the parahippocampal gyrus, which is then dissected. The fimbria is laterally dissected to expose the hippocampal sulcus and the Ammon's horn arteries. The hippocampal feeders can be coagulated, and the hippocampus and parahippocampus can now be resected en bloc. Posterior hippocampal structures may be aspirated [43]. After hemostasis, closure is done to finish the procedure.

3.3 The Selective Amygdalohippocampectomy

3.3.1 Transsylvian Approach

The beginning of the transsylvian approach is by the opening of the Sylvian fissure. The sharp dissection should be performed during the whole opening of the Sylvian fissure, except the thickened arachnoid bands, which should be divided with micro-scissors or tenotome. A delicate aspirator on moist Cottonoid sponges can be used. The exposure is medial to the Sylvian veins from the carotid bifurcation to the middle cerebral artery bifurcation and beyond to expose the anterior one-third of the insula and 1–2 cm of the M2 segments.

The next step is to identify the lateral branches of the M1 segment. The inferior trunk of the M2 is followed in the insular limiting sulcus pars inferior and gently mobilized to allow coagulation and division of 2–5 perforating branches entering here. At this point, where these small branches were coagulated, a small incision (1–2 cm) was performed anteromedial to the M2 segment. This incision opens the UF. In the majority of the cases, this incision is localized between the temporepolar and anterior temporal arteries. At this level, in the most anterior part of the incision, the amygdala is found few millimeters in-depth by using the surgical aspirator. With

the tip of a delicate dissector, the temporal horn of the lateral ventricle was entered a little bit posteriorly. This maneuver is useful to orientation regarding the entire amygdala. The next step is the removal of the amygdala. Special attention must be given to avoid a medial basal extension, which can cause a lesion in the optic tract. This structure should be identified. After that, the parahippocampal gyrus is removed subpially. The “extratemporal amygdala” is not removed. The pial and arachnoid membranes adjacent to the carotid cistern and ambient cistern were identified after subpial resection of the anterior part of the parahippocampal gyrus. These membranes were opened, exposing the uncal and anterior choroidal arteries, entering the choroidal fissure. At this stage, the following structures were identified: optic tract, the basal vein of Rosenthal, cerebral peduncle, third nerve, posterior cerebral artery (P1 and P2 segments), and posterior communicating artery. The next step was the removal of the hippocampus, for which the microscope was turned posteroinferiorly. The temporal horn was opened 2 cm posteriorly from its tip, exposing the trigone and plexus choroid. The choroid plexus is displaced medially to identify the tela choroidea and the choroidal fissure. The tela choroidea was opened to visualize the taenia fimbria of the lateral peduncle. The lateral branches of the anterior choroidal artery were divided, but the main stem and the medial branches must always be preserved. The parahippocampal gyrus was displaced laterally after the opening of the choroidal fissure to visualize the P2 segment, posteromedial choroidal artery, and collicular artery. The Ammon’s horn arteries arise from the P2 segment and anterior choroidal artery and enter the sulcus hippocampus just proximal to the origin of the posterolateral choroidal artery. These arteries are coagulated and sectioned. The hippocampus was transected transversally at the level of the posterior rim of the cerebral peduncle, where the P2 bifurcates to form the inferolateral and superomedial trunks. The hippocampal veins and inferior ventricular veins, and the parahippocampal veins into the collateral sulcus, were sectioned. The most posterior part of the optic tract and the lateral geniculate body can be found at the level of P2–P3 bifurcation. This is the local where the fimbria ascends to become the crus of the fornix. The next step was the gentle spreading and opening of a sulcus in the floor of the temporal horn lateral to the hippocampus, which is an extension of the collateral eminence. This sulcus was opened anteroposteriorly in the direction of the peduncle where the rhinal and collateral sulci are found. The vessels originating from the inferolateral trunk (P3) supplying the parahippocampus were sectioned. The other vessels must be preserved. The parahippocampus was elevated and resected en bloc via the subpial plane. If there is no deep mesial herniation, the tentorium can be visualized. The neurovascular structures are protected by the pia and a double-layer arachnoid. The resected specimen has approximately 4 cm length, 1.5 cm breadth, and 2 cm depth [52]. Careful hemostasis is performed, the dura is closed, and the bone flap is replaced.

3.3.2 Transtemporal (Niemeyer's Technique)

Transtemporal selective amygdalohippocampectomy is a transcortical technique to reach the amygdala and the hippocampal formation through the temporal lobe. It was first described by the Brazilian neurosurgeon Paulo Niemeyer, who used T2 (middle temporal gyrus) to perform the cortical incision [43]. Nevertheless, the transtemporal technique encompasses further possibilities for primary incision nowadays, including the anterior part of the superior temporal gyrus and the superior temporal sulcus [53]. To better enlighten the procedure, our description sticks to Niemeyer's technique, the most commonly used.

After a temporal craniotomy and removing the bone flap and inferior reflection of the dura, an incision was performed at the middle temporal gyrus. The skin incision is made anterior to the tragus and above the zygoma. The entry point must be no farther than 3.5 cm from the temporal tip at the dominant hemisphere. The cortical incision, planned to be 2 cm, is where the endopial dissection is made to initiate the approach to the temporal horn. To guide the pathway, the use of neuronavigation can help [54, 55]. The use of neuronavigation optimizes the bone exposure for later cortical opening, indicating the optimal craniotomy point [43].

When the temporal horn was accessed, brain retractors were used to enhance the temporal horn exposition. The resection of mesial temporal structures began after an entry at the parahippocampal gyrus, at its most ventrolateral surface, and advanced to the uncus, medially situated. After removing these structures, the edge of the tentorium and the basal cisterns were viewable, allowing the amygdalectomy to be performed [54, 55].

The next step was focused on the removal of the hippocampus. Choroid plexus and choroidal fissure were identified. The medial and superior limit of the resection was the choroidal fissure, and the posterior limit was at the level of the posterior part of the body of the hippocampus. Starting from the finished amygdalectomy, the resection progressed posteriorly up to the tectal plate. The hippocampal tail was then removed alongside the hippocampal lateral margin, isolating the main structure. Only then can the body of the hippocampus be dissected, usually through suction technique. While small hippocampal vessels must be coagulated, small branches of the choroidal artery and posterior cerebral artery must be preserved, to which the surgeon should pay considerable attention. Finally, after inspection and hemostasis, the dura might be closed, followed by bone flap, temporalis muscle, and scalp [54, 55].

3.3.3 Subtemporal Technique

The subtemporal technique is another transcortical method to perform selective amygdalohippocampectomy. Tomokatsu Hori developed it at the beginning of the 1990s. Since then, several amendments have been proposed, such as the subtemporal

transparahippocampal amygdalohippocampectomy (described below), but the general original idea remains the same [43].

A temporal craniotomy was performed. In this procedure, the craniotomy (8 cm × 5 cm flap) is performed so that the sphenoid bone is exposed and removed. After opening the dura, a retractor was placed under the uncus. Afterward, the anterior uncus was elevated to inspect the fusiform, parahippocampal gyri, tentorium, and ambient cistern. This access, for its positional features, requires the cerebrospinal fluid to be drawn [53].

The cortical incision was made at the uncus. The oculomotor nerve was identified at the ambient cistern, offering a reference for this cut (10–15 mm posteriorly). Suction excision of cortex and white matter opened the way to the temporal horn. Once the amygdala shapes the temporal horn anterosuperior wall, it becomes exposed through the former procedure. An incision at the parahippocampal gyrus cleared the way to the anterior hippocampus [53]. The rest of the procedure follows the same technique of the transsylvian approach.

Subpial aspiration split the amygdala from the hippocampus, previously connected through a thin layer of neural tissue. The parahippocampal gyrus around the inferolateral hippocampus must be removed for the later removal of the hippocampus itself. Two centimeters of the anterior hippocampus are then sectioned. Hippocampal arteries, branches from anterior choroidal and posterior cerebral arteries, must be coagulated. Using suction and a bipolar cautery, an additional 1 cm of the hippocampus is removed. Only then is the amygdala resected. For that, an ultrasonic aspirator might be used [53].

The main advantage of the subtemporal technique is the absence of incision at the temporal stem and temporal neocortex [53]. Hori argues that this benefit potentially preserves cognitive functions [54]. However, negative aspects of the procedure have been raised, such as an imminent risk for the vein of Labbé and the limited sight of the aimed structures [53, 54].

3.4 Anterior Temporal Lobectomy (ATL) Versus Selective Amygdalohippocampectomy (SAH)

The two main surgical approaches for mesial temporal epilepsy are still subject to debate once no standardized criteria have shown the superiority of one of the procedures convincingly. Performing a meta-analysis involving 626 patients, Kuang et al. [56] found no difference in seizure control nor verbal memory deficits in 1 year postoperatively. A comparative meta-analysis concluded that ATL improved the chance to accomplish seizure-free conditions but did not measure neuropsychological outcomes [57]. This agrees with the meta-analysis of Hu et al. [58], in which ATL showed better chances to control seizure frequency. In this work, IQ scores

were similar between ATL and SAH patients. In an 18-year follow-up study, Hemb et al. [59] evaluated 108 patients and stated that the surgical technique does not interfere with the seizure control rate.

Analyzing a postoperative 5 years, Malikova et al. [60] observed similar seizure control between ATL and SAH, but better results in SAH for memory deficits and visual field defects, besides a lower amygdala and hippocampal volume reduction. This is in concordance with the study of Witt et al., in which they showed that memory preservation is related to hippocampal integrity after surgical treatment for mesial temporal epilepsy [61].

Wendling et al. [62] assessed 60 patients completely seizure-free after 7 years from epilepsy surgery and found that visual encoding, verbal short-term memory, visual short-term memory, and visual working memory were better in SAH patients. The percentage of patients that reached seizure-free state was slightly higher among ATL patients, while the quality of life was somewhat superior in SAH patients, but both were not statistically significant.

Since the mesial temporal lobe processes facial emotional recognition, it is reasonable to wonder what implication mesial temporal surgeries have on this matter. Wendling et al. [63] investigated 60 patients (ATL = 33; SAH = 27) and 30 healthy control subjects with the Ekman 60 faces test. All individuals had similar scores recognizing surprise, happiness, anger, and sadness. SAH patients scored poorer for disgust, while ATL patients had the worse scores for fear recognition.

We still do not have an absolute answer for what surgical approach should be the first choice for mesial temporal epilepsy patients. Although some studies show that ATL has a slightly enhanced chance to free the patient from seizures, others establish better neuropsychological outcomes for SAH. Ecological neuropsychological tests and further outcome evidences are necessary to consider indication criteria. In the meantime, the choice should be based on an individualized assessment of the patient and the surgeon's evaluation of the scenario.

4 Illustrative Cases

Figures 21, 22, 23, 24, and 25 show radiological, surgical, and anatomical images of temporal surgeries as practical examples of anatomical knowledge applied to microneurosurgery.

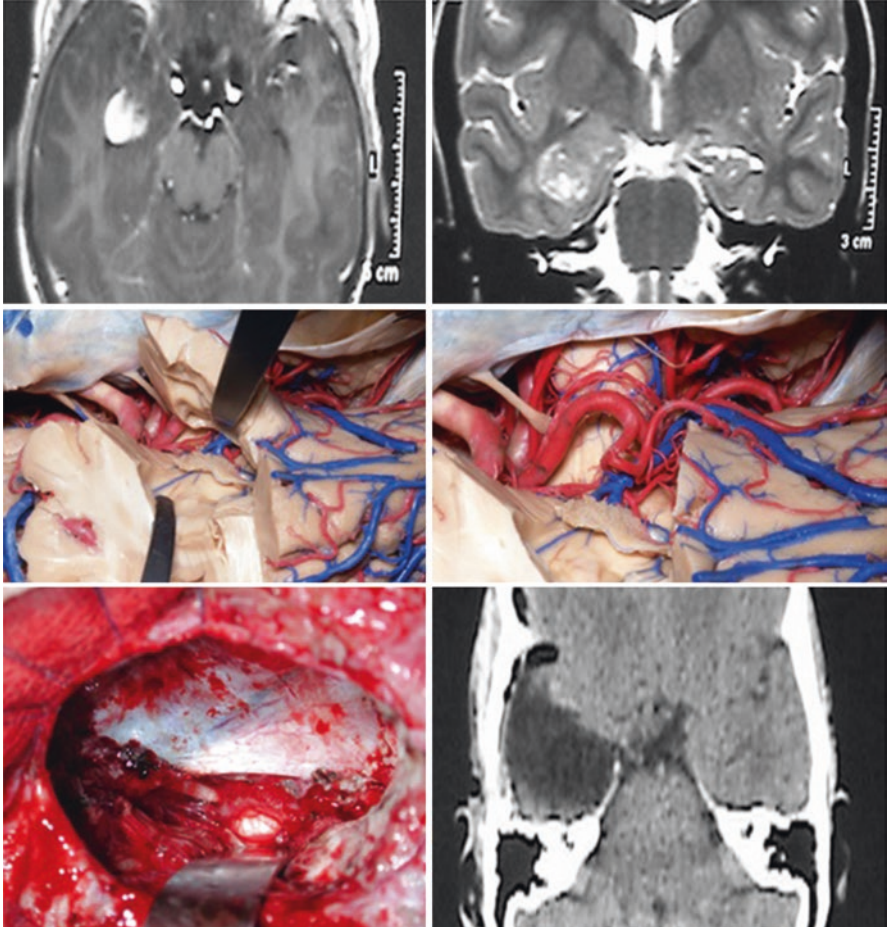


Fig. 21 Right-sided temporal ganglioglioma in a pediatric patient with drug-resistant temporal lobe epilepsy. The patient submitted to standard anterior temporal lobectomy. Excellent epilepsy outcome (Engel 1) in a 10-year follow-up

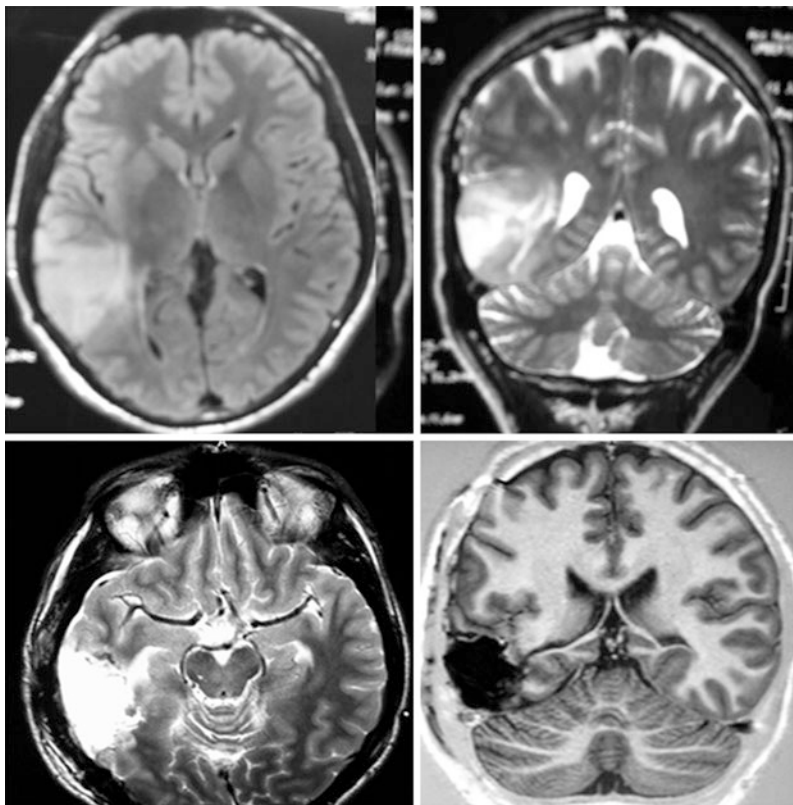


Fig. 22 Right-sided posterior temporal low-grade glioma. Surgery achieved total resection. The patient had postoperative right-sided temporal hemianopia. This case in which intraoperative brain mapping of the optic radiation could have been done with awake surgery

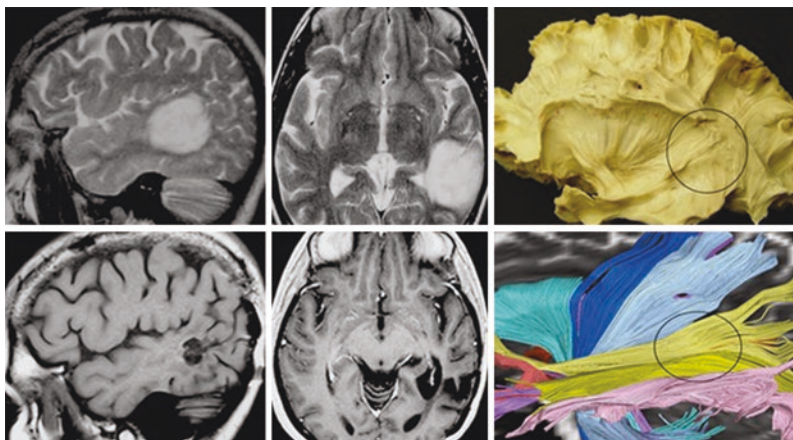


Fig. 23 Left-sided posterior temporal low-grade glioma. Total resection was achieved through the middle temporal gyrus with the preservation of optic radiations

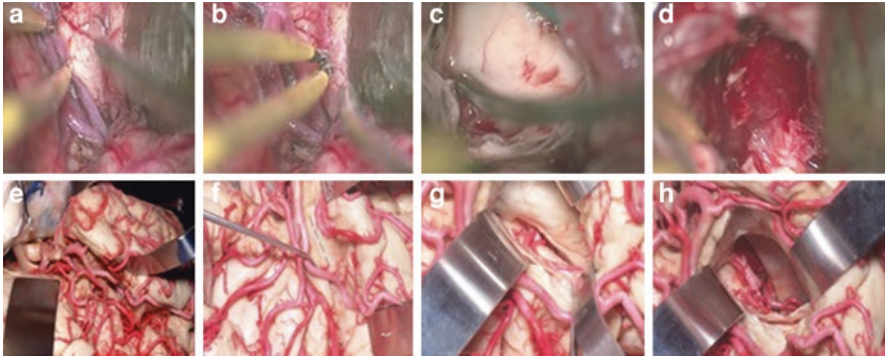


Fig. 24 Selective transsylvian amygdalohippampectomy. (a) Opening of Sylvian fissure; (b) T2 corticectomy; (c) opening of the temporal horn of lateral ventricle to perform amygdalohippampectomy; (d) surgical site after complete resection of mesial temporal structures; (e–h) are the same previously described stages, respectively, performed in a microanatomical laboratory

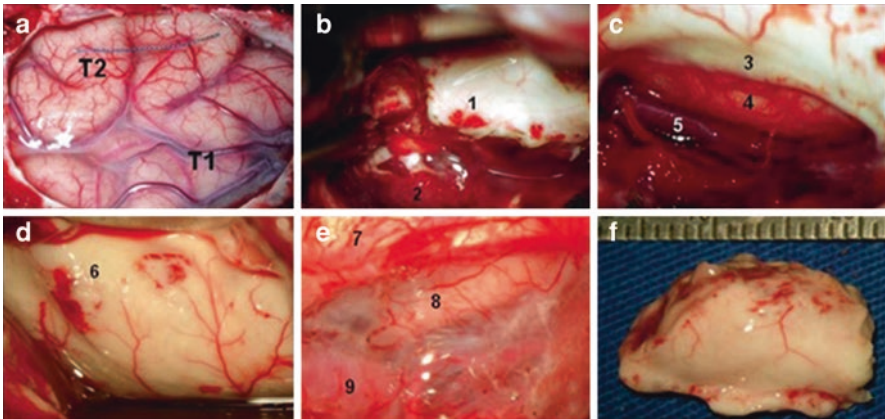


Fig. 25 Surgical stages of right-sided Niemeyer's selective amygdalohippampectomy (except a (left side)). (a) Exposition of superior temporal gyrus; (b) resection of the amygdala after reaching the temporal horn of lateral ventricle; (c) opening of choroid fissure to expose vascular structures of the ambient cistern; (d) normal-sized hippocampus with its digitations; (e) preserved arachnoid and visualization of ambient and crural cistern structures (see-through); (f) en bloc hippocampal resection; 1—head of the hippocampus; 2—choroid plexus; 3—fimbria-fornix; 4—parahippocampus; 5—posterior cerebral artery; 6—hippocampal digitations; 7—cerebellar tentorium; 8—oculomotor nerve; 9—posterior cerebral artery (P2 segment). (Reprinted from Isolan et al. [63])

5 Conclusion

Although the different techniques applied in managing temporal lobe epilepsy have a similar degree of success, some may have more complications than others. Except for transsylvian and subtemporal techniques, all others have great potential of quadrantanopia due to optic radiation damage. Usually, this is, however, an incidental campimetry finding and not referred to by the patient as an issue. The subtemporal

approach, although more anatomical, has the risk of injury to the vein of Labbé and, as a result, temporal lobe venous infarction. The transsylvian approach, also very anatomical, must be precisely performed through the planum polare to avoid damage on the IFOF in the temporal stem or even Meyer's loop. Overall, the best surgical approach for temporal lobe diseases is often the one with which the surgeon is best adapted.

References

1. Téllez-Zenteno JF, Hernández-Ronquillo L. A review of the epidemiology of temporal lobe epilepsy. *Epilepsy Res Treat.* 2012;2012:630853. <https://doi.org/10.1155/2012/630853>. Epub 2011 Dec 29.
2. Vellutini E, Garzon E, Inuzuka KM, Brock RS, Dal 'Col Lucio JE. Epilepsy surgery. In: Ramina R, Aguiar PH, Tatagiba M, editors. *Samii's essentials in neurosurgery*. Berlin: Springer-Verlag; 2014. p. 493–506.
3. Yasargil MG, Türe U, Yasargil DC. Impact of temporal lobe surgery. *J Neurosurg.* 2004;101(5):725–38. <https://doi.org/10.3171/jns.2004.101.5.0725>.
4. Gloor P. *The temporal lobe and limbic system*. New York: Oxford University Press; 1997.
5. Ono M, Kubik S, Abernathy CD. *Atlas of the cerebral sulci*. Stuttgart: Thieme; 1990.
6. Yasargil MG. *Microneurosurgery IV A*. Stuttgart: Thieme; 1994.
7. Duvernoy HM. *The human brain, surface, blood supply, and three-dimensional sectional anatomy*. 2nd ed. Vienna: Springer-Verlag; 1999.
8. Broca P. Anatomie comparée des circonvolutions cérébrales: le grand lobe limbique. *Annu Rev Anthropol.* 1878;1:385–498.
9. Klingler J. Die makroskopische anatomie der Ammonsformation. *Denkschr Schweiz Naturforsch Ges.* 1948;78:1–80.
10. Blackstad TW. Commissural connections of the hippocampal region in the rat, with special reference to their mode of termination. *J Comp Neurol.* 1956;105:417–537.
11. Retzius G. *Das Menschenhirn—Studien in der makroskopischen morphologie*. Stockholm: Kgl. Buchdr; 1896.
12. Isolan GR, Stefani MA, Schneider FL, Claudino HA, Yu YH, Choi GG, Telles JPM, Rabelo NN, Figueiredo EG. Hippocampal vascularization: proposal for a new classification. *Surg Neurol Int.* 2020;11:378. https://doi.org/10.25259/SNI_708_2020.
13. Erdem A, Yaşargil G, Roth P. Microsurgical anatomy of the hippocampal arteries. *J Neurosurg.* 1993;79(2):256–65. <https://doi.org/10.3171/jns.1993.79.2.0256>.
14. Marinković S, Milisavljević M, Puskas L. Microvascular anatomy of the hippocampal formation. *Surg Neurol.* 1992;37(5):339–49. [https://doi.org/10.1016/0090-3019\(92\)90001-4](https://doi.org/10.1016/0090-3019(92)90001-4).
15. Wen HT, Rhoton AL Jr, de Oliveira E, Cardoso AC, Tedeschi H, Baccanelli M, Marino R Jr. Microsurgical anatomy of the temporal lobe: part 1: mesial temporal lobe anatomy and its vascular relationships as applied to amygdalohippocampectomy. *Neurosurgery.* 1999;45(3):549–91; discussion 591–2. <https://doi.org/10.1097/00006123-199909000-00028>.
16. LeDoux JE, Damasio AR. Emotions and feelings. In: Kandel ER, Schwartz JH, Jessell TM, Siegelbaum SA, Hudspeth AJ, editors. *Principles of neural science*. 5th ed. New York: McGraw-Hill; 2013. p. 1079–94.
17. Bernasconi N, Bernasconi A, Caramanos Z, Antel SB, Andermann F, Arnold DL. Mesial temporal damage in temporal lobe epilepsy: a volumetric MRI study of the hippocampus, amygdala and parahippocampal region. *Brain.* 2003;126(Pt 2):462–9. <https://doi.org/10.1093/brain/awg034>.
18. Nagata S, Rhoton AL Jr, Barry M. Microsurgical anatomy of the choroidal fissure. *Surg Neurol.* 1988;30(1):3–59. [https://doi.org/10.1016/0090-3019\(88\)90180-2](https://doi.org/10.1016/0090-3019(88)90180-2).

19. Isolan GR, de Oliveira E, Recalde R. Estudo microanatômico da fissura coroidéia na abordagem dos ventrículos e cisternas cerebrais [Microanatomical study of the choroidal fissure in ventricular and cisternal approaches]. *Arq Neuropsiquiatr*. 2005;63(3B):801–6. Portuguese. <https://doi.org/10.1590/s0004-282x2005000500015>. Epub 2005 Oct 18.
20. Flechsig P. *Anatomie des menschlichen Gehirns und Rückenmarks auf Myelogenetischer Grundlage*. Leipzig: Thieme; 1896.
21. Meyer A. The connections of the occipital lobes and the present status of the cerebral visual affections. *Trans Assoc Am Phys*. 1907;22:7–1.
22. Cushing H. The field defects produced by temporal lobe lesions. *Brain*. 1922;44:341–96.
23. Tusa RJ, Ungerleider LG. The inferior longitudinal fasciculus: a reexamination in humans and monkeys. *Ann Neurol*. 1985;18(5):583–91. <https://doi.org/10.1002/ana.410180512>.
24. Choi C, Rubino PA, Fernandez-Miranda JC, Abe H, Rhoton AL Jr. Meyer's loop and the optic radiations in the transsylvian approach to the mediobasal temporal lobe. *Neurosurgery*. 2006;59(4 Suppl 2):ONS228–35; discussion ONS235–6. <https://doi.org/10.1227/01.NEU.0000223374.69144.81>.
25. Sincoff EH, Tan Y, Abdulrauf SI. White matter fiber dissection of the optic radiations of the temporal lobe and implications for surgical approaches to the temporal horn. *J Neurosurg*. 2004;101(5):739–46. <https://doi.org/10.3171/jns.2004.101.5.0739>.
26. Ribas EC, Yagmurlu K, Wen HT, Rhoton AL Jr. Microsurgical anatomy of the inferior limiting insular sulcus and the temporal stem. *J Neurosurg*. 2015;122(6):1263–73. <https://doi.org/10.3171/2014.10.JNS141194>. Epub 2015 Apr 10.
27. Párraga RG, Ribas GC, Welling LC, Alves RV, de Oliveira E. Microsurgical anatomy of the optic radiation and related fibers in 3-dimensional images. *Neurosurgery*. 2012;71(1 Suppl Operative):160–71; discussion 171–2. <https://doi.org/10.1227/NEU.0b013e3182556fde>.
28. Ribas EC, Yağmurlu K, de Oliveira E, Ribas GC, Rhoton A. Microsurgical anatomy of the central core of the brain. *J Neurosurg*. 2018;129(3):752–69. <https://doi.org/10.3171/2017.5.JNS162897>. Epub 2017 Dec 22.
29. Duffau H, Gatignol P, Moritz-Gasser S, Mandonnet E. Is the left uncinate fasciculus essential for language? A cerebral stimulation study. *J Neurol*. 2009;256(3):382–9. <https://doi.org/10.1007/s00415-009-0053-9>. Epub 2009 Mar 6.
30. Vanacôr CN, Isolan GR, Yu YH, Telles JPM, Oberman DZ, Rabelo NN, Figueiredo EG. Microsurgical anatomy of language. *Clin Anat*. 2021;34(1):154–68. <https://doi.org/10.1002/ca.23681>. Epub 2020 Sep 23.
31. Tate MC, Herbet G, Moritz-Gasser S, Tate JE, Duffau H. Probabilistic map of critical functional regions of the human cerebral cortex: Broca's area revisited. *Brain*. 2014;137(Pt 10):2773–82. <https://doi.org/10.1093/brain/awu168>. Epub 2014 Jun 25.
32. Duffau H. Stimulation mapping of white matter tracts to study brain functional connectivity. *Nat Rev Neurol*. 2015;11(5):255–65. <https://doi.org/10.1038/nrneurol.2015.51>. Epub 2015 Apr 7.
33. Duffau H. Toward the application of the hodotopical concept to epilepsy surgery. *World Neurosurg*. 2011;75(3–4):431–3. <https://doi.org/10.1016/j.wneu.2010.12.012>.
34. De Benedictis A, Duffau H. Brain hodotopy: from esoteric concept to practical surgical applications. *Neurosurgery*. 2011;68(6):1709–23; discussion 1723. <https://doi.org/10.1227/NEU.0b013e3182124690>.
35. Baciú M, Perrone-Bertolotti M. What do patients with epilepsy tell us about language dynamics? A review of fMRI studies. *Rev Neurosci*. 2015;26(3):323–41. <https://doi.org/10.1515/revneuro-2014-0074>.
36. Yasargil MG. *Microneurosurgery I*. Stuttgart: Thieme; 1984.
37. Wen HT, Rhoton AL Jr, de Oliveira E, Castro LH, Figueiredo EG, Teixeira MJ. Microsurgical anatomy of the temporal lobe: part 2—sylvian fissure region and its clinical application. *Neurosurgery*. 2009;65(6 Suppl):1–35; discussion 36. <https://doi.org/10.1227/01.NEU.0000336314.20759.85>.
38. Yasargil MG. *Microneurosurgery IV B*. Stuttgart: Thieme; 1996.

39. Yasargil MG, Wieser HG. Selective microsurgical resection. In: Wieser HG, Elger CE, editors. *Presurgical evaluation of epileptics*. New York: Springer-Verlag; 1987. p. 352–60.
40. Yasargil MG, Krisht AF, Türe U. Microsurgery of insular gliomas: part II: opening of the sylvian fissure. *More Contemp Neurosurg*. 2002;24(12):1–5.
41. Isolan GR, Aguiar PHP, Aires R, Meister C, Stefani MA. Middle cerebral artery pseudo-tetrafurcation: anatomic report and review of middle cerebral artery variations. *Neurosurg Q*. 2010;20(4):284–7.
42. Horsley V. Brain surgery. *Br Med J*. 1886;2(1345):670–7. <https://doi.org/10.1136/bmj.2.1345.670>.
43. Al-Otaibi F, Baesa SS, Parrent AG, Girvin JP, Steven D. Surgical techniques for the treatment of temporal lobe epilepsy. *Epilepsy Res Treat*. 2012;2012:374848. <https://doi.org/10.1155/2012/374848>. Epub 2012 Mar 22.
44. Yeni SN, Tanriover N, Uyanik O, Ulu MO, Ozkara C, Karağaç N, Ozyurt E, Uzan M. Visual field defects in selective amygdalohippocampectomy for hippocampal sclerosis: the fate of Meyer's loop during the transsylvian approach to the temporal horn. *Neurosurgery*. 2008;63(3):507–13; discussion 513–5. <https://doi.org/10.1227/01.NEU.0000324895.19708.68>.
45. Van Gompel JJ, Welker KM. Visual field mapping to prevent visual field deficits in epilepsy surgery: seeing the problem. *Neurology*. 2014;83(7):578–9. <https://doi.org/10.1212/WNL.0000000000000701>. Epub 2014 Jul 11.
46. Rubino PA, Rhoton AL Jr, Tong X, de Oliveira E. Three-dimensional relationships of the optic radiation. *Neurosurgery*. 2005;57(4 Suppl):219–27; discussion 219–27. <https://doi.org/10.1227/01.neu.0000176415.83417.16>.
47. Yogarajah M, Focke NK, Bonelli S, Cercignani M, Acheson J, Parker GJ, Alexander DC, McEvoy AW, Symms MR, Koepp MJ, Duncan JS. Defining Meyer's loop-temporal lobe resections, visual field deficits and diffusion tensor tractography. *Brain*. 2009;132(Pt 6):1656–68. <https://doi.org/10.1093/brain/awp114>. Epub 2009 May 21.
48. Chen X, Weigel D, Ganslandt O, Buchfelder M, Nimsky C. Prediction of visual field deficits by diffusion tensor imaging in temporal lobe epilepsy surgery. *NeuroImage*. 2009;45(2):286–97. <https://doi.org/10.1016/j.neuroimage.2008.11.038>. Epub 2008 Dec 16.
49. Borius PY, Roux FE, Valton L, Sol JC, Lotterie JA, Berry I. Can DTI fiber tracking of the optic radiations predict visual deficit after surgery? *Clin Neurol Neurosurg*. 2014;122:87–91. <https://doi.org/10.1016/j.clineuro.2014.04.017>. Epub 2014 May 5.
50. Von Der Heide RJ, Skipper LM, Klobusicky E, Olson IR. Dissecting the uncinat fasciculus: disorders, controversies and a hypothesis. *Brain*. 2013;136(Pt 6):1692–707. <https://doi.org/10.1093/brain/awt094>. Epub 2013 May 6.
51. Kucukyuruk B, Richardson RM, Wen HT, Fernandez-Miranda JC, Rhoton AL Jr. Microsurgical anatomy of the temporal lobe and its implications on temporal lobe epilepsy surgery. *Epilepsy Res Treat*. 2012;2012:769825. <https://doi.org/10.1155/2012/769825>. Epub 2012 May 21.
52. Gonçalves-Ferreira A, Miguéns J, Farias JP, Melancia JL, Andrade M. Selective amygdalohippocampectomy: which route is the best? An experimental study in 80 human cerebral hemispheres. *Stereotact Funct Neurosurg*. 1994;63(1-4):182–91. <https://doi.org/10.1159/000100313>.
53. Park TS, Bourgeois BF, Silbergeld DL, Dodson WE. Subtemporal transparahippocampal amygdalohippocampectomy for surgical treatment of mesial temporal lobe epilepsy. *Technical note J Neurosurg*. 1996;85(6):1172–6. <https://doi.org/10.3171/jns.1996.85.6.1172>.
54. Burchiel KJ, Zacest AC, Spencer D. Selective amygdalohippocampectomy. In: Winn HR, editor. *Youmans neurological surgery*. 6th ed. Philadelphia: Elsevier; 2011.
55. Isolan GR, Azambuja N, Paglioli Neto E, Paglioli E. Anatomia microcirúrgica do hipocampo na Amígdalo-hipocampectomia seletiva sob a perspectiva da técnica de Niemeyer e método pré-operatório para maximizar a corticotomia [Hippocampal microsurgical anatomy regarding the selective amygdalohippocampectomy in the Niemeyer's technique perspective and pre-operative method to maximize the corticotomy]. *Arq Neuropsiquiatr*. 2007;65(4A):1062–9. Portuguese. <https://doi.org/10.1590/s0004-282x2007000600031>.

56. Kuang Y, Yang T, Gu J, Kong B, Cheng L. Comparison of therapeutic effects between selective amygdalohippocampectomy and anterior temporal lobectomy for the treatment of temporal lobe epilepsy: a meta-analysis. *Br J Neurosurg.* 2014;28(3):374–7. <https://doi.org/10.3109/02688697.2013.841854>. Epub 2013 Oct 7.
57. Josephson CB, Dykeman J, Fiest KM, Liu X, Sadler RM, Jette N, Wiebe S. Systematic review and meta-analysis of standard vs selective temporal lobe epilepsy surgery. *Neurology.* 2013;80(18):1669–76. <https://doi.org/10.1212/WNL.0b013e3182904f82>. Epub 2013 Apr 3.
58. Hu WH, Zhang C, Zhang K, Meng FG, Chen N, Zhang JG. Selective amygdalohippocampectomy versus anterior temporal lobectomy in the management of mesial temporal lobe epilepsy: a meta-analysis of comparative studies. *J Neurosurg.* 2013;119(5):1089–97. <https://doi.org/10.3171/2013.8.JNS121854>. Epub 2013 Sep 13.
59. Hemb M, Palmi A, Paglioli E, Paglioli EB, Costa da Costa J, Azambuja N, Portuguez M, Viuniski V, Booiij L, Nunes ML. An 18-year follow-up of seizure outcome after surgery for temporal lobe epilepsy and hippocampal sclerosis. *J Neurol Neurosurg Psychiatry.* 2013;84(7):800–5. <https://doi.org/10.1136/jnnp-2012-304038>. Epub 2013 Feb 13.
60. Malikova H, Kramska L, Vojtech Z, Liscak R, Sroubek J, Lukavsky J, Druga R. Different surgical approaches for mesial temporal epilepsy: resection extent, seizure, and neuropsychological outcomes. *Stereotact Funct Neurosurg.* 2014;92(6):372–80. <https://doi.org/10.1159/000366003>. Epub 2014 Oct 28.
61. Witt JA, Coras R, Schramm J, Becker AJ, Elger CE, Blümcke I, Helmstaedter C. Relevance of hippocampal integrity for memory outcome after surgical treatment of mesial temporal lobe epilepsy. *J Neurol.* 2015;262(10):2214–24. <https://doi.org/10.1007/s00415-015-7831-3>. Epub 2015 Jul 3.
62. Wendling AS, Hirsch E, Wisniewski I, Davanture C, Ofer I, Zentner J, Bilic S, Scholly J, Staack AM, Valenti MP, Schulze-Bonhage A, Kehrli P, Steinhoff BJ. Selective amygdalohippocampectomy versus standard temporal lobectomy in patients with mesial temporal lobe epilepsy and unilateral hippocampal sclerosis. *Epilepsy Res.* 2013;104(1–2):94–104. <https://doi.org/10.1016/j.eplepsyres.2012.09.007>. Epub 2012 Sep 28.
63. Wendling AS, Steinhoff BJ, Bodin F, Staack AM, Zentner J, Scholly J, Valenti MP, Schulze-Bonhage A, Hirsch E. Selective amygdalohippocampectomy versus standard temporal lobectomy in patients with mesiotemporal lobe epilepsy and unilateral hippocampal sclerosis: post-operative facial emotion recognition abilities. *Epilepsy Res.* 2015;111:26–32. <https://doi.org/10.1016/j.eplepsyres.2015.01.002>. Epub 2015 Jan 16.